[redacted]

FINAL REPORT

CONTRACT NAS-23758

SOFT X-RAY POLYCHROMATOR

FOR THE

SOLAR MAXIMUM MISSION

DECEMBER 1984

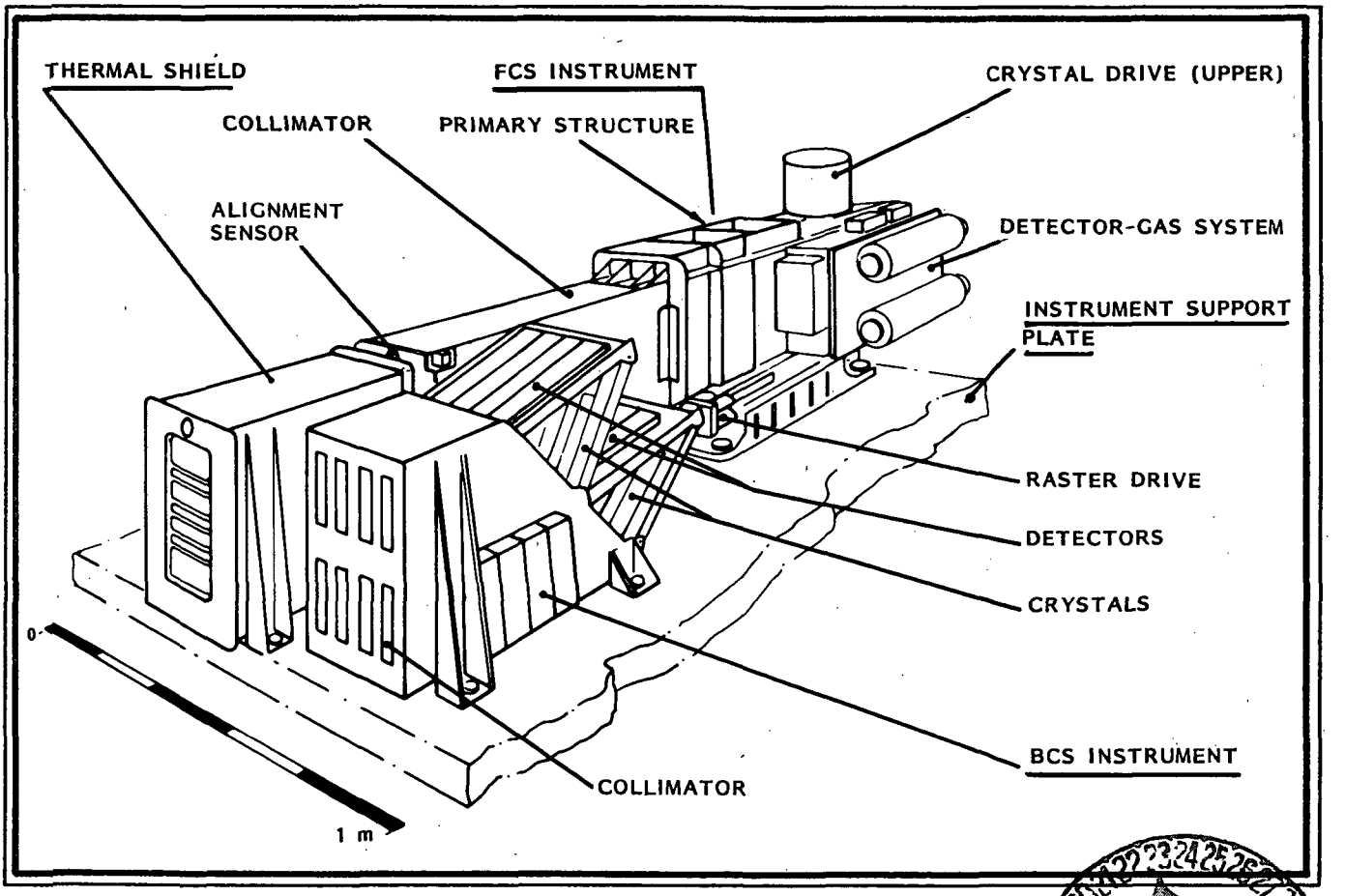

Prepared for

NASA GODDARD SPACE FLIGHT CENTER

by

LOCKHEED PALO ALTO RESEARCH LABORATORY

FINAL REPORT

Contract NAS5-23758

SOFT X-RAY POLYCHROMATOR

FOR THE

SOLAR MAXIMUM MISSION

DECEMBER 1984

Prepared for
Goddard Space Flight Center
SMM Project Office

by

B. M. Haisch
M. Levay
R. A. Stern
K. T. Strong
C. J. Wolfson
and
L. W. Acton

Lockheed Palo Alto Research Laboratory
Dept. 91-20, Bldg. 255
3251 Hanover Street
Palo Alto, California 94304

Table of Contents

1. Introduction and Historical Perspective.....3

2. Science Objectives.....5
2.1 Scientific Background.....5
2.2 Scientific Objectives.....6
2.3 Instrument Design Criteria.....7
2.4 The Flat Crystal Spectrometer.....9
2.5 The Bent Crystal Spectrometer.....10
2.6 Summary.....11

3. Operational Experience.....12
3.1 Staff at the EOF.....12
3.2 Description of Normal Operations.....14
3.3 Observing Sequences.....16
3.4 Other Instrument Activities.....18
3.5 Instrument Health and Status.....20
3.6 Other Operations Activities.....25

4. Scientific Results.....27
4.1 Flare Observations and Results.....27
4.2 Active Region Observations and Results.....30
4.3 Quiet Sun Observations and Results.....31
4.4 Atomic Physics Results.....32
4.5 Absolute Calibration of the FCS.....33

5. Acknowledgements.....34

Figure Captions.....36
Figures.....38

Appendix A: SMM Bibliography.....47

Appendix B: EOF Staff.....62
Sample XRP Timeline.....65
Sample XRP Log.....66
XRP 15 Channel Light Curve.....67
FCS PHA Calibration Plots.....68
BCS PHA Calibration Plots.....69
BCS Position Calibrations.....70
FCS PHA Study Plots.....71
Sample Raster Slip Log.....72
Y-Transducer vs. SAE Calibration Plot.....73
Z-Transducer vs. SAE Calibration Plot.....74
Sample Crystal Drive Use Log.....75
FCS Gas Supply Status Summary: System A.....77
FCS Gas Supply Status Summary: System B.....78
FCS Gas Usage Rate Time Plots.....79
FCS Total Gas Usage vs. Time Plots.....80
Sample Weekly Activity Report.....82

Appendix C: Data Submission Plan for the NSSDC.....83

1. INTRODUCTION AND HISTORICAL PERSPECTIVE

During the early 1970's various scientific advisory committees recommended that a space mission dedicated to study of the solar flare phenomenon be conducted during the next maximum in the solar activity cycle (1979). A solar flare is a highly energetic, spectacular, and complex event producing emissions that span the electromagnetic spectrum from gamma rays, through the visible spectrum, to kilometric radio wavelengths. As such, its study requires a coordinated, multi-instrument approach. NASA accepted these recommendations and in February 1974 issued an Announcement of Opportunity for participation in the Solar Maximum Mission (SMM).

Three groups, who had extensive interest and experience in solar X-ray spectroscopy, decided to join forces to propose an investigation which included an ambitious set of flight instrumentation called the "X-Ray Polychromator." These groups and their respective Principal Investigators were L. W. Acton of Lockheed Palo Alto Research Laboratory (LPARL), J. L. Culhane of Mullard Space Sciences Laboratory (MSSL), and A. H. Gabriel of Rutherford Appleton Laboratory (RAL). LPARL and MSSL had cooperated in several previous solar X-ray investigations: these included an experiment on the Orbiting Solar Observatory (OSO-8) and rocket experiments. RAL also had space hardware experience and, more importantly, brought expertise in the discipline of theoretical X-ray spectroscopy to the team. The proposed XRP investigation and instrumentation thus represented a culmination of the long term interests and commitments of the three groups. By forming a three institutional consortium, a more complex instrument and overall program was proposed than would have been possible by any one of the individual groups.

The proposal, titled "A Versatile 1-23 A X-Ray Polychromator for the Study of Flares and Related Phenomena for the Solar Maximum Mission" was submitted in June 1974. It was the only proposal for an investigation in this energy range that was selected by NASA for further definition. A major feature of the XRP proposal was the

acknowledgement that to obtain the desired temporal, spatial, and spectral resolutions in this part of the X-ray spectrum would require two different, but highly complementary instruments. These were called the FCS (for Flat Crystal Spectrometer or Finely Collimated System) and BCS (for Bent Crystal Spectrometer or Broadly Collimated System), and had the characteristics indicated by these names.

Although ambitious in scope, the XRP instrumentation did not represent really new technology, rather it was an extension of existing technologies at the three institutions. The tasks involved in developing the XRP were divided among the three groups equally. LPARL was responsible for the high-precision FCS collimator, for the microcomputer-based command and data handling systems, for the power system, and for overall integration and test of the XRP. MSSL was responsible for the detection systems (including the FCS gas flow system and the BCS position sensitive detectors) and for all of the BCS mechanical and thermal elements except the crystals. RAL was responsible for the sophisticated FCS raster and crystal drives, for the overall FCS structure, and for obtaining and mounting both the FCS and BCS crystals.

Phase I of the XRP program ran for about six months, beginning in the Spring of 1975. A report titled "Phase I Scientific and Technical Report" dated September 1975 summarizes the accomplishments of this initial definition study. NASA then awarded a Phase II study to the XRP consortium. This more detailed instrument definition study lasted about a year and is summarized in a document titled "Phase II Instrument Description and Technical Report" dated December 1976. Upon evaluation of the instrument definition and the plans for instrument development which the XRP consortium presented, NASA elected to go forward with development of the XRP. In just over two years (January 1979), the XRP was ready and delivered to GSFC for integration into the SMM spacecraft. Thirteen months after that (February 14, 1980), the SMM was placed into orbit and the XRP began scientific operation.

Highlights of this very active 3 1/2 year development phase are given in the "Final Report (Part I) for the Soft X-Ray Polychromator for the SMM" dated April 1980.

In addition to developing the XRP instrumentation, the three groups participated equally in making plans for orbital operations and scientific analysis. This, of course, involved producing extensive software. It also included participation in the Experiment Operations Facility (EOF) at GSFC where science observations were planned and conducted. Thus, members of the XRP teams began moving to GSFC in July 1979 and by launch we had an XRP resident staff of about 20 people at the EOF. Instrument operations took place with a high level of intensity until November 1980 (see Section 3) when the Spacecraft fine pointing system failed. Several of the XRP scientists remained at the EOF, which had become the focal point for SMM science activities, for an additional year or two. By late summer of 1982 everyone had returned to their home institutions. However this situation happily changed as plans developed for the on-orbit repair of SMM, and team members began moving back to GSFC in the Fall of 1983. By the time the repair was accomplished (April 1984) the XRP resident team consisted of about 10 persons. The XRP is now again collecting the scientific data for which it was designed.

2. SCIENCE OBJECTIVES

2.1 Scientific Background

Solar flares are explosive events, occuring within magnetically active regions, that result in electromagnetic radiation and particle accelerations and involve energies that may exceed 10^{32} ergs in some cases. Visible flare radiation represents only a small part of the flare emission, and moreover is not a manifestation of the primary energy release process. Direct detection of high velocity particle streams is possible, but only at great distances from the source of origin on the Sun; flare accelerated particle streams in the solar atmosphere may be inferred from radio burst data, but in general

without any spatial resolution of the flare process, although some radio data now do have high spatial resolution capability.

Various flare models have been proposed all of which involve the release in some fashion of energy stored in magnetic fields. Since it is not possible to observe the topology and rapid evolution of magnetic fields directly on the spatial and temporal scale of the flare process, the XRP was conceived principally to observe an immediate and directly related manifestation of magnetic energy release: the creation of hot, soft X-ray emitting plasmas.

2.2 Scientific Objectives

The SMM X-ray polychromator experiment was designed to investigate the characteristics and evolution of solar plasmas formed in the 1.5-50 million degree K temperature regimes of solar flares and active regions. The primary scientific objectives of the XRP investigation at the outset of the Solar Maximum Mission were:

(1) To study in detail the pre-flare state of the plasma and the development of active regions, so as to identify features peculiar to the build-up of the flare instability within active regions;

(2) By observing the flaring plasma to determine the relative importance of energetic non-thermal particles, shocks or other forms of mechanical energy input and to investigate the thermalization process;

(3) In the post-flare plasma to examine the roles of conduction, radiation, expansion and dilution in the flare decay process.

Furthermore we anticipated that observations with the XRP would contribute to basic knowledge in spectroscopy, atomic structure, and plasma physics processes in general; an additional objective of the XRP program was thus:

(4) To investigate in detail the 1-23 A spectrum in order to improve our theoretical knowledge of the atomic physics of high temperature, low density plasmas and to establish diagnostic tools for such solar plasmas.

We add that the post-repair objectives have been redirected to some extent to carry out observations of the now relatively quiescent sun. Some of the new, post-repair objectives are discussed in section 4.

2.3 Instrument Design Criteria

When the XRP was designed ten years ago, very little was known about the X-ray spectra of flares. Still it was felt that high spectral resolution emission line spectroscopy offered the best opportunity to study the plasma physics and dynamics of solar flares; this approach seemed to afford the best way to resolve the flare process as a function of plasma temperature. Furthermore, high resolution spectroscopy offered the best hope of studying the mass motions and mechanical turbulence in flares through the study of line profiles and Doppler shifts of the X-ray lines.

Since the conflicting demands of spectral, spatial and temporal resolution could not be met by a single instrument, the XRP was designed as a coordinated, dual-instrument experiment: the Flat Crystal Spectrometer (FCS) and the Bent Crystal Spectrometer (BCS). The FCS achieves moderate spatial and good spectral resolution at some sacrifice to temporal capability; conversely the BCS provides good spectral and temporal resolution, but only with spatial resolution adequate to isolate a single active region. However the coarse collimation of the BCS allows it to monitor activity over an entire active region to ensure that an event from the selected region will not be missed; it can therefore be used to issue an alert to the FCS that an event is starting up.

These instruments were designed to work in unison to derive the characteristics of the coronal plasma during a flare from soft X-ray

(1-23 A) emission lines. The FCS is also sufficiently sensitive in its softest channels to spatially map the active regions that produce the flares, and is consequently able to investigate the relationship between the state of the active region evolution and its flare productivity. Data from these instruments are directly comparable with results from various atomic theory calculations; such comparisons enable us both to improve the theory and to better understand the diagnostic capabilities of various lines.

For plasmas at active region and flare temperatures the two most abundant elements, hydrogen and helium are completely ionized. The most prominent X-ray emission of such a high temperature, low density solar plasma comes from other highly, but not completely, ionized species such as oxygen, neon, magnesium, silicon, sulfur, calcium and iron. The high binding energy of the innermost 1s electrons implies that one and two electron ions of these species will be particularly dominant: that is, ions in the hydrogen- and helium-isoelectronic sequences. Because of their prominence in the emission spectrum and the diagnostic capabilities that have been developed for these ions, the XRP was designed to concentrate on the hydrogen- and helium-like lines of these species.

This region of the spectrum includes the resonance lines of the hydrogen- and helium-like ions of most of the abundant species listed above. In addition to these resonance lines all of the helium-like ions have two adjacent lines: a $1s^2\ ^1S$ - $1s2p\ ^3P$ intersystem line and a $1s^2\ ^1S$ - $1s2s\ ^3S$ forbidden line. This helium-like group -- resonance (R), intersystem (I), and forbidden (F) -- is extremely useful because the ratios of these lines have been studied in detail theoretically and density and optical depth diagnostics have been established.

Density measurements based on line ratios are independent of volume filling factors, and so are a direct measure of the plasma condition. Densities may also be determined from the differential emission measure of the plasma; simultaneous measurement of collisionally excited lines originating at different temperatures by the XRP and

knowledge (from atomic physics) of the intrinsic emissivity of a given line together allow determination of the combined "density-filling factor" as a function of temperature for the plasma. The line ratio densities are independent of the filling factor, and thus the two types of measurements are highly complementary and in some cases may be used to infer the sizes of emitting structures.

The same helium-like transitions occur in a lithium-like ion, except that the addition of an outer electron decreases the potential energy of the inner electrons: such transitions are called inner-shell transitions to differentiate this process from the customary production of spectral lines via transitions involving the outermost electron. The resulting three-electron helium-like lines are called satellite lines, since they are shifted only slightly in wavelength from the two-electron lines. This process is not limited to helium-like transitions nor to the addition of only a single outer electron, but the helium-like inner-shell resonance lines are particularly important. Some satellite lines are excited by the process of dielectronic recombination, with the consequence that the satellite to two-electron resonance line ratio is a function of electron temperature -- providing a powerful temperature diagnostic. Finally, the intensity ratios of satellite lines excited in lithium-like ions by normal collisions (as opposed to dielectronic recombination) to the two-electron resonance line provide a measure of the ionization state of the plasma. This in turn provides an ionization "temperature." If this temperature is higher or lower than the electron temperature derived from the dielectronic satellite line, this indicates that the plasma is out of equilibrium and is either ionizing or recombining respectively -- reflecting strong heating or cooling.

2.4. The Flat Crystal Spectrometer

The FCS consists of 7 Bragg Crystal spectrometers that have the capability of scanning the spectrum and/or mapping the target region. The wavelength range of the FCS is shown in Figure 1. The FCS

concentrated on the spectral region 1.4-22.4 A. The FCS in its home position was designed to simultaneously observe the line centers of the hydrogen-like O VIII resonance line and the helium-like Ne IX, Mg XI, Si XIII, S XV, Ca XIX and Fe XXV resonance lines for a small region (14" square) of the Sun; unfortunately due to the relatively large uncertainty in the true wavelength of the line at the time of FCS fabrication, the Ca XIX line is offset from the home position. By rastering over a selectable area of the Sun, maps of the emission topology and evolution of solar structures are obtained simultaneously for the seven different temperatures at which the home position lines form. In the spectral scanning mode, the intensities of other lines and the line profiles of the home position and other lines may be obtained by the FCS.

2.5 The Bent Crystal Spectrometer

The BCS provides simultaneous spectra in eight channels; these channels include the line positions and profiles of the Fe K-alpha lines, the line profiles of hydrogen-like Fe XXVI and helium-like Fe XXV and Ca XIX, and other weaker lines. High temporal resolution of the line fluxes and line profiles is obtained for an active region-sized area on the Sun.

The BCS concentrates specifically on the narrow spectral region (1.77-1.95 A) which includes, among others, the two Fe K-alpha lines. When atoms are bombarded by energetic electrons, one result is ionization via removal of an inner, usually K-shell, electron. This leaves the atom in an excited state and as a result an outer electron drops down to fill the K-shell vacancy. The energy of this transition may go into emission of an X-ray photon (called fluorescence) or into expulsion of an outer electron (the Auger process).

When the BCS was designed it was thought that the occurrence of K-alpha emission would be indicative of non-thermal excitation by energetic electrons; it was expected that the wavelength of the K-alpha line would reflect the ionization of the parent atom and thus

provide information on where in the atmosphere the non-thermal electrons are being stopped. However the BCS measurements revealed that on the Sun K-alpha is primarily excited by photospheric fluorescence from hard X-rays. Some evidence for beam-excited K-alpha was seen in the BCS data but high spatial resolution will be required to discriminate against the fluorescent component for such measurements to be definitive.

The two other principal ions of interest which have lines in this spectral region are helium-like Fe XXV and hydrogen-like Fe XXVI. This wavelength regime is covered by subsets of seven channels; in addition there is a single longer wavelength channel at ~ 3.2 A to observe helium-like Ca XIX. The BCS contiuously monitors this spectrum with relatively high resolution (both spectral and temporal) in 8 independent spectrometers. The complete set of BCS spectra from a flare is shown in Figure 2.

2.6 Summary

In summary, the XRP was designed to measure the following temporal and spatial properties of the active and flaring Sun: electron temperature, departures from steady state, ion kinetic temperatures, and electron density. The BCS is capable of measuring the broadening and blue shifts often observed in the impulsive phase of flares. The six simultaneous line fluxes indicative of six different tempertures of formation observable by the FCS allow us to derive the differential emission measure of the plasma at each raster point. During the operational periods of the XRP (1980 and 1984) we have observed hundreds of flares of C-level (GOES classification) and brighter in both the FCS and BCS, including 5 X-flares. Finally, associated theoretical work in atomic physics, stimulated in part by the promise of XRP measurements, has benefitted from the experimental data on solar plasmas which the XRP has, in fact, provided in abundance.

3. OPERATIONAL EXPERIENCE

This section contains a description of the operations oriented activities performed by the staff at the Experiment Operations Facility in building 7 at GSFC during the reporting period. A summary of the current instrument status is also included. Appendix B contains graphs, tables and other supporting material. Neither this section nor appendix B is intended to be complete and should be considered an overview of XRP operations. Periodic, detailed reports of instrument and operations status are made to the home institutions (MSSL, RAL, and LPARL). Copies of these reports are available to NASA on request.

3.1 Staff at the Experiment Operations Facility (EOF)

The operational experience during SMM I (Feb. - Dec. 1980) affected the approach used during the repaired mission (SMM II). Although there are more similarities than differences, the paragraphs that follow highlight the differences. Appendix B contains a list of the EOF staff personnel.

3.1.1 SMM I Operations

- Science/Ops/Engineering:

  During SMM I little distinction was made between science, operations and engineering tasks. As a result, job assignments were made on a personnel-available basis, with the effect that an operations-oriented computer programming assignment was just as likely to be accomplished by a scientist as by an engineer or a programmer. The only personnel with clear, well defined job responsibilities were the Data Technicians who were employed to perform tape processing and command generation tasks.

- Weekly Rotations:

  The Science Planners were changed once per week on SMM I. The rationale behind this was that all Co-Investigators should have an opportunity to plan a week's observations. The result was frequent errors in the command generation activity because no Science Planner had enough experience to become familiar with "the system". The Data Tech's were also rotated from Command Generation to Quick-Look Tape Processing jobs on a weekly basis. Though the result of this approach was somewhat less

confusing than was the case with the Science Planner rotation, the effect was that the Data Tech did not become "expert" in either job.

- o Quick-Look Evaluation Performed by Science Staff:

  The evaluation task was a scientist's responsibility on SMM I. The evaluator for a given week had been the planner the previous week. This was a direct offshoot of the lack of a differentiation between science and operational issues: Since a scientist was required to do detailed evaluation of a flare, he had to handle all aspects of the evaluation tasks (e.g. did all detectors switch on as planned; did the micro processors execute the proper sequence?).

- o Plan Forms Were Hand-Written:

  The path of information from SMM Observing Plan, to XRP Observing Plan, to command loads, to evaluation of data involved a number of retranscriptions from one handwritten form to another. This resulted in a number of errors and a fair amount of difficulty in ascertaining whether operations were consistent with plans.

3.1.2 Current SMM II Operations

- o Instrument Operations Team (IOT):

  Toward the end of the previous mission, there came recognition of the need for some separation between instrument operations and science planning and evaluation. This new philosophy has been implemented for SMM II. Day to day operations tasks (command generation, data base management, tape processing, data management, etc.), engineering tasks, and computer programming efforts to support the above have been assigned to a six person group named the Instrument Operations Team (IOT). The rationale behind the IOT is manifold; but the two most important reason are to establish responsibility for and to produce genuine continuity of expertise in these areas.

- o Data Tech Assignments Fixed:

  In keeping with the desire for continuity, Data Tech assignments are fixed, (i.e. there is a Command Generator and a Quick-Look Tape Processor).

- o Top Level Evaluation Handled by IOT:

  The responsibilities of the IOT person in charge of tape generation has been expanded to include the top level operations evaluation.

- Science planner rotation:

  The science planner changes monthly, with responsibility rotating between the three laboratories in the XRP Consortium.

- Reduction in operator intensive activities:

  There now being a programmer dedicated full time to operations oriented functions, a number of improvements have been made and are continuing to be made to operations support programs. Some of these are called out in section 3.6.

- Computer aided generation of plans:

  Planning forms are now computer generated. There is a program that reads a file that contains orbital information and generates a "blank form" for a given operations day. The planner then types the specifics of the plan onto the form. This gives the command generator and the evaluator ready access to a clean, readable, and accurate synopsis of the days planned activities.

3.2 Description of Normal Operations

XRP is an operational experiment on an operational satelite. The major function of the EOF staff is to carry out routine command and evaluation tasks on a daily basis. The sections that follow give an overview of the operations scenario.

3.2.1 Planning and command generation

Normally science and engineering plans are generated Mondays (for 3-days) and Thursdays (for 4-days). The science plans reflect decisions made at SMM planning meeting. Engineering plans are driven by regularly scheduled status and maintainance activities (e.g. motor lubrication sequence, detector calibrations, etc.) as well as more specialized requirements (e.g. detector background tests). While plans are made for several days, revisions are often made on a daily basis as the solar forecast or instrument condition dictate. The plan is typed onto a planning form. This form is used by the command generator to formulate the daily microprocessor and command loads. A sample planning form is shown in appendix B.

The command generation task itself is computer aided and takes place partly on PDP 11-34 computers in the EOF and partly on the building 14 Command Management System via remote terminals in the EOF. The computer programs on the 11-34 allow the command generator to compose new sequences for BCS and FCS by editing text files and submitting them to a process which error-checks the sequence, generates microprocessor loads, and transmits these loads to the CMS system via a communications link. The CMS system is used by the command generator to build Real Time Sequences (RTS's), by which the On Board Computer (OBC) will activate observing sequences, and load directives, which correlate RTS activations to absolute time. Output listings produced by CMS are signed off by the science planner. The command generation task is one that involves reasonable proficiency on different computer systems and requires well developed organization skills.

3.2.2 Quick-look tape dump and evaluation

XRP data are received directly in the EOF on a PDP 11-34 mini computer. The data are stored on an RA81 disk unit, which can hold up to 60 hours of data. Data are dumped to tape nominally once per day. A single tape reel can hold up to 28 hours of XRP data, but 24 hour tapes are usually made. All XRP evaluation programs use magnetic tape as input, i.e., no near-real-time evaluation is performed.

Once a Quick-Look tape has been made, the data evaluator runs a set of standard programs that list instrument status parameters and also generates a plot of X-ray counts in all operating detectors (12 channel light curves). The evaluator checks the status listing to verify instrument health and also compares it to the plan. In addition, areas of particular interest (e.g. high count rates on the light curve) are reformatted for more detailed evaluation. Programs that produce FCS and BCS single channel light curves, BCS and FCS spectrum plots, and FCS contours are among those used for such evaluation. A contour plot of the most recent FCS raster map is normally produced for science planning.

3.3 Observing Sequences

Both the BCS and the FCS are micro-computer controlled instruments. As a result, they are capable of being programmed to execute a great variety of observing sequences. This section groups the sequences actually used into several classes and gives a brief description of the function of each.

3.3.1 BCS

Four sequences have been generated for the BCS:

- o All bins, normal time resolution... ID 10.0.15.0:

  This sequence collects data from all operating BCS detectors at the natural time resolution (i.e. 7.65 second). This is the most commonly used BCS sequnce.

- o All bins, high time resolution... ID 11.1.15.0:

  This sequence collects data from all operating BCS detectors at twice the natural time resolution (i.e. 3.8 seconds). This is used as a flare response to sequence 10.0.15.0, and can collect up to 7 minutes of high time resolution data.

- o No redundancy sequence, normal time resolution... ID 12.0.15.0:

  The BCS detectors contain redundant coverage of some wavelengths (albeit at different spectral resolution). This sequence eliminates the high resolution coverage to obtain higher time resolution (4.3 seconds). This sequence is seldom used.

- o No redunancy sequence, High time resolution... ID 13.1.15.0:

  This sequence is the flare response to sequence 12.0.15.0, and collect up to 7 minutes of 2.2 second time resolution data with no redundant spectral coverage.

3.3.2 FCS

The following list describes some of FCS observing sequences used during the reporting period:

o Standard Rastering Sequences:

These are the most common sequences used. Typical rastering sequences execute in one of the following ways:

- Raster continuously at a fixed size for the duration of an orbit day.

- Raster to find an X-ray bright point then take data for the remainder of the orbit at the bright point.

- Raster to find a bright point and contine rastering around the bright point for the duration of the orbit.

o Surveys:

Surveys are a special case of raster sequences. Survey sequences are of 3 main types:

- Active region surveys. These are used for planning purposes when there is more than 1 active region on the disk.

- East limb surveys. These are used for planning purposes as well. The idea is to try to observe coronal structures above the limb before an active region rotates onto the disk.

- Diachronic surveys. A series a spacecraft repointings and rolls are used to obtain coronal X-ray data above the limb for one complete solar rotation. The purpose of this sequence is to generate a one rotation X-ray map to compare with similar data taken by the Coronagraph Polarimeter.

Surveys are similar to standard rastering sequences but require time synchronization with spacecraft repointing commands.

o Sequences Preliminary to Crystal Usage:

Since the primary drive failed in 1980, a certain amount of care is taken to be certain that the backup drive is used only if the FCS is pointed at a flaring region. A standard procedure is used in conjunction with potential use of the FCS crystal drive. The standard startup sequence is as follows:

- A 3 arc minute square raster is executed to find an X-Ray bright point.

- Once a bright point is found, the BCS flare flag is enabled (i.e. the FCS is informed via an interrupt if the BCS observes a flare in its 6 arc minute field of view).

- The FCS performs a survey raster (5 arc minutes square) then continues 3 arc minute rasters at the bright point.

- If a BCS flare occurs anytime after step 1, the FCS does a rapid bright point find around the original bright point.

- If the new bright point has sufficient counts, the crystal drive is turned on and spectra are taken.

The threshold required for crystal sequence activation varies with the spectral sequence that is planned.

o Spectral scans:

The FCS Crystal Drive is considered a limited-life resource (see paragraph 3.5). As such, FCS spectral scans occur only in cases where the probability of valuable scientific return is judged to be high by the XRP science staff at the EOF. FCS spectra have been taken on seven occasions.

- Active region spectral data is initatied on a pre-programmed basis when the science staff beleives the X-ray emission from the region is sufficient to warrant the use of the crystal drive. Five such scans have been performed. These were all in the active period in late April and early May 1984. One of the data sets is forever lost because of problems with the spacecraft tape recorder.

- Flare spectra can be taken if the criteria in the standard startup sequence are satisfied (item 3 above). One such automatic sequence has occurred in the reporting period.

- In September 1984, home position spectra were taken at 576 positions in and surrounding a coronal hole.

3.4 Other Instrument Activities

3.4.1 Detector Calibrations

BCS detector calibration are done regularly in a programmed fashion. Position and Pulse Height Analyzer (PHA) calibrations are each done on alternate Thursdays. FCS detector calibrations require crystal drive motion as the calibration sources are located behind the crystal bank. As a result, only 2 FCS detector calibrations have been performed. Detectors are discussed further in paragraph 3.5.1

3.4.2 Raster Calibration

The FCS raster system uses a pairs of motor driven cams (one each for pitch and yaw) to point the FCS collimator to a nominal accuracy of 5

arc seconds. The actual position of the collimator is determined by the output of transducers that measure the strain in each axis. A special sequence was run in May 1984 to obtain the correlation between motor position and transducer value for each position in the operating range (+/- 3.5 arc minutes).

3.4.3 FCS Detector Background

FCS detectors report two counting rates that indicate the number of events in two energy bands, the broader of the two completely containing the narrower. The difference between the two counting rates is used to functionally determine the average background rate. The correlation between the count rates and background demands that data be taken at times when there is (effectively) no X-ray flux coming into the detector(s). During the first mission, background determination was made during a few specific intervals by pointing the instrument at areas of quiet sun; now FCS background determination has become a regular program. In addition to quiet sun, off-limb pointings and night-time (earth eclipse) observations data are taken on a regular basis to ascertain if there is a (relatively) short term variation in FCS backgound parameters. The background subtraction software has also been improved to allow incorporation of such short term effects.

During SMM I, our ability to take FCS background data at night had been seriously compromised by the tendency of the FCS thin window detector to drop out. The XRP team determined that a possible cause for these drop-outs was the ingression of plasma into the detector/high-voltage area through FCS gas system vent pipe access hole. This hole was covered by a baffle during the repair mission. There have been no detector drop-outs during night time periods since the repair mission.

3.4.4 PHA Study

The XRP electronics contains a 31 channel pulse height analyzer that is used for detector calibrations. In an effort to better understand the FCS background signature, quiet sun, active region, and non-solar (e.g. night-time and off-limb) observations have been made with the FCS operating in PHA mode. There have been no final conclusions and this effort is continuing. A change to the FCS micro-processor code has been worked out that would allow PHA and normal science data to both appear in the data stream. If the PHA study indicates this would be useful, this patch will be loaded sometime in the near future. Appendix B contains some annotated plots of data from this project.

3.4.5 Detector Gain Tests

The XRP team has been concerned for some time about the response of FCS detector 1. One possible reason for discrepencies between expected and actual counting rates has been the detector high voltage gain. This detector has been run at the lowest possible gain setting since the beginning of the first mission because higher gain settings produce occassional break-down (excessively high counting rates). During one of the FCS calibrations, detector 1 was run for a time at normal gain and exhibited no problems. As a result, its gain setting has been left at normal. The results have been somewhat puzzling because not only was background reduced (as expected) but the counting rate observed in flares and active regions was also reduced (unexpected). Understanding of this situation should be improved with the next FCS flare crystal scan.

3.5 Instrument Health and Status

3.5.1 Detectors

- o BCS:

  During SMM I, BCS detectors 2 and 8 failed. The six remaining BCS detectors continue to operate normally. Calibrations have

shown no change other than the expected decrease in count rate caused by decay of the calibration sources. Sample BCS calibration are in appendix B.

- FCS:

  Toward the end of the SMM I mission, FCS detector 6 (Ca XIX) was showing signs of impending failure. A special set of pre-repair tests in June 1983 showed that this detector had ceased to function in a useful manner. The remaining 6 FCS detectors continue to operate nominally. The gain of detector 1 (O VIII) has been adjusted from low gain to normal gain. Detector 2 has been tested at higher gain, and no breakdowns were observed. No decision has been made on permanently switching detector 2 to high gain.

  Unlike the BCS, FCS detectors are not calibrated on a regular basis. This is because the crystal drive has to activated to expose the calibration sources. There have been a total of three detector calibrations in the reporting period. Sample calibration plots are shown in appendix B.

  Two FCS detector calibrations were performed in May 1984. The first set of calibrations showed significant differences from calibrations run in 1980. Investigation of the problem revealed that the PHA gain settings used for some detectors were incorrect. Calibrations were rerun and the detectors showed no significant differences from the 1980 data.

  On 17 August, detectors 2 and 4 were inadvertently turned on when the gas system for these detectors was off. This condition was corrected after approximately six hours. Because there was a possibility that the detectors had been damaged by this event, another FCS calibration was run on 24 August. The detectors proved to be undamaged.

3.5.2 Raster System and Slip History

The FCS pointing system is operated by stepper motors. The electronics system runs in an open loop manner, so when a motor does not respond properly to a step command, the planned area of observation slips in the field of view. There is a processing routine in the FCS micro-processor that corrects the field of view to the nominal boresight on every orbit night. The XRP evaluation procedures include a program that lists raster positions every orbit night and at each SAA entry (i.e. at times when the system is quiescent). A log file of raster slips is maintained on the Data Analysis Center (DAC) VAX computer which is located in the EOF area. Currently FCS image data

are not routinely corrected for raster slips. A sample page for the Raster Slip Log is contained in appendix B.

There have been three major episodes of raster slips. During the period of mid-May through late June, raster slips occurred regularly. A set of procedures were discovered that seemed to minimize and eventually nearly eliminate slips. This procedure included moving the raster quickly to the edges of the maximum normal operating range (+/- 3.5 arc minutes) prior to initiating a series of rasters. The idea behind this approach was that it would help smooth out areas of dry lubricant build-up in and around the motor shaft bearings. This was apparently successful; though there was a second episode of slips in July, this was minor by comparison (i.e. 1 or 2 per calendar day) and was short-lived (approximately two weeks). Recently a third episode of slips began occurring in early November, and is coincident with a change made to the crystal start-up sequence. Efforts to correct the current problems are continuing. There is a backup cam for each axis, and these will be used if the current problems persist.

3.5.3 Crystal Drive (Usage log and misread summary)

The FCS primary crystal drive motor failed after less than one month of operation in the first mission because the encoder lamp went "open circuit". Changes in supply voltage readings as well as drive behavior substantiate this conclusion. Prior to failure, there was an increasing tendency of the drive to misread addresses. Misreads are identified by apparent changes in direction during the time the drive is moving through a relatively large angle. Because the primary drive failed after less than 5% of its expected lifetime, the operations approach to drive-usage was changed from continuous spectroscopic scanning to scanning only when expectations of good scientific return was high (see section 3.3.2 above). This conservative approach has continued in SMM II.

In order to determine if the redundant drive is nearing failure (assuming it fails in the same manner as the primary drive), all

crystal motions are carefully analyzed with an eye towards reversals or changes in time required to acquire a commanded position. All crystal motions, their durations, address range, and anomalies are cataloged in a file maintained on the DAC VAX computer. Appendix B contains a listing of the crystal log file. The most recent use of the drive show some misreads (see the log). Comparing the misread frequency with that of the primary drive, there are between 100 and 200 hours of on-time remaining on the drive.

3.5.4 Gas

The FCS thin window detectors (detectors 1-4) contain propane which is supplied from a pair of gas systems; each system services two detectors. Since the gas reservoir is in the liquid state (i.e. it operates at the vapor pressure of liquid propane), there is no direct measure of the remaining supply. During the first mission, little time was spent determining the gas reserve as the mission had operated for considerably less than the designed lifetime up to the point of spacecraft failure. During SMM II there has been a concerted effort to determine the gas remaining in each system by refering to pre-launch lab measurements and performing calculations from first principles. There are two methods of estimating gas expenditure:

- o Puff Counts:

  A digital monitor counter increments each time the gas solenoid valve opens, putting a "puff" of gas into the system. Mass per puffs is estimated from the number of puffs required to fill the detectors (a known volume). Gas expended is determined by total number of puffs used in the mission.

- o Leak Rate:

  Each time the gas system is turned off, the pressure slowly decays. The rate of presure decrease can be used to determine a leak rate (in mass per unit time). This rate is multiplied times the total system on-time to determine the amount of gas used.

Both of these method have been used, and while they give somewhat different results, they are close enough to give one confidence that the calculations are correct.

The results (shown in Appendix B) show that system B (detectors 2 and 4) has a markedly shorter expected lifetime (by a factor of 10!) from that of system A. As a result, the general gas usage policy is to leave system A on continuously. System B is turned on only while the science staff determines such action is warranted by solar activity level.

3.5.5 Alignment Sensors

The FCS contains 5 white light alignment sensors (one central detector and 4 limb detectors). These are used to determine XRP alignment relative to the spacecraft and to other instruments on SMM. There was a continuous degradation of the response of these sensors during the first mission and there was a fear that this would seriously compromise the ability to determine absolute FCS pointing. Such has not been the case as the degradation of the sensors appears to have bottomed out.

3.5.6 Micro-processors

When the FCS crystal drive was turned off following the crystal drive test sequence on 7 June, the BCS micro-processor ceased to operate. Several unsuccessful attempts were made to restart the micro, after which it was reloaded with the full hardware load. This type of problem had been observed before (i.e. FCS crystal drive power on/off effecting the BCS micro); however, this is the first time a reload was required. This was the only problem associated with either the BCS or FCS micro-processors in the reporting period.

3.6 Other Operations Activities

The following paragraphs highlight other projects and activities of the XRP staff at the EOF.

3.6.1 Improvements to Command generation and Evaluation Procedures

One of the major deficiencies in the first mission was the lack of programming talent specifically assigned to operations oriented tasks. Because there is an IOT programmer and also because the individual hired for the tape production/data evaluation task has good programming skills, a number of improvements have been made to operations support software. The overall result has been that the data evaluation as a whole is less operator-intensive and frees the staff for other projects, including other computer programming tasks. The following list contains some of the major software enhancements made during the review period.

- Quick-look tape production man interface more natural (entry is now in start time and duration... rather than record numbers);
- OBC words left off Q/L tapes so 24 hours/tape and one tape per day;
- Top level evaluation programs run simultaneously so only one pass through tape required (i.e. less time);
- Crystal turn-on's detected by tape processing program to speed up flyback analysis;
- BCS Light Curves require less human input;
- FCS contour maps more integrated into VAX system and cause no problems;
- 15 channel light curve program modified to eliminate non-functioning detector giving higher resolution;
- Missing data flagged by status program.

3.6.2 Production Tape Processing

XRP considers that data gathered at the EOF is for Quick-Look evaluation and analysis, and that the final data product is the set of production tapes sent by IPD to each XRP home institution and to the EOF. During the first mission, these tapes were eventually processed through top level evaluation programs at MSSL in England. The difficulty in this approach was not only the time lag, but the less than optimal processing as the programs to do this evaluation were being improved at the EOF, i.e., MSSL was always using old versions of the software. During SMM II, production tape processing is done at the EOF by IOT staff members.

In the early stages of the mission, IPD tapes were almost unusable because real-time pass data and tape recorder dump data were sent on different tapes. (During SMM I there were two operating tape recorders. As a result, tape recorder plyback data contained the entire data stream. In SMM II, one recorder has failed, so realtime data is required to fill in those periods when the recorder is being dumped.) IPD now sends "merged" tapes. Because it was several months before merged tape began arriving, production tape processing at the EOF has lagged behind where we had hoped it would be. The turn around time in tape processing is improving and should be two months by early 1985.

3.6.3 Flare Catalog

The NOAA support staff at the EOF produced an event catalog for SMM I. The same is planned for SMM II. The XRP input to this catalog had been hand-written. To speed up the XRP input to the NOAA catalog, a set of programs has been developed to assist in its generation. The XRP flare catalog contains more XRP information than appears in the final NOAA catalog. The software support program includes the capability to search events based on numerous criteria, e.g. maximum intensity, duration, etc.

3.6.4 Instrument Status Reports

The IOT issues periodic reports to the home institutions that document in detail instrument activities and status. Three such reports were issued during the reporting period.

3.6.5 Weekly PI report

A summary of EOF activities is sent via TWX to the three XRP PI's. Additional copies are sent to each home institution. A sample report in contained in appendix B.

4. SCIENTIFIC RESULTS

The XRP experiment has collected data on the solar corona for a total of 18 months since the launch of the SMM on 14 February 1980. Prior to the repair mission we had several years to analyse the data from SMM-I which enabled us to examine critically the early XRP results and to establish priorities for the second mission, which is presently underway. The first mission, which only lasted 10 months and during which there were few big flares on the Sun, did produce a number of interesting results from the two XRP instruments. For a complete list of all the XRP groups' publications to date see Appendix A. In the section below we decribe the scientific results and observations obtained so far and describe some of plans that we have for using the XRP to build on this knowledge during SMM-II. The topics have been arranged in several categories according to the level of solar activity. The XRP was primarily designed to look at flare plasmas in the solar corona but has sufficient sensitivity to examine less energetic phenomena.

4.1 Flare Observation and Results

The XRP observed over 700 bright flares during SMM-I (including 93 M-flares and 6 X-flares). An interesting feature is that at least 40% of them have multiple soft X-ray peaks. This can be an important

effect energetically as was shown by Strong et al 1984. The relative importance of various energetics terms such as mass motions can be altered if the energy from the flare burst is absorbed into hot dense coronal plasma rather than into the cooler plasma of the transition region or chromosphere. This same work established that the release point was most probably in the corona, later supported by a HXIS study of a limb flare by Simnett and Strong 1984, and that loops differing in length by more than an order of magnitude were involved in the onset of a flare. This later conclusion supports the idea that flares are a result of the interaction of loop systems as a result of photospheric motions (shear or flux emergence).

We have looked at the buildup of energy in an active region before the flare. Several studies have also been done that involve preflare brightenings, such as the one on the Queens' Flare by de Jager et al. There have been some interesting advances in this area recently; P. Waggett in conjunction with the HXIS group (G. Simnett and R. Harrison) believes that these "precursors" may in fact be the forerunner of a coronal mass ejection (CME) and that the main flare is merely a spin-off of the massive energy release involved in a CME. This work is still in progress.

The BCS, with its fine time resolution (<11s) and good spectral resolution, has been able to measure the broadening and blue shifts often observed in the impulsive phase of flares (see Figure 3). Antonucci, primarily, has looked at the energetics of this kinetic component in comparison with that of the non-thermal electrons and thermal coronal plasma. She has found that, within observational uncertainties, these components balance and are compatible with the chromospheric evaporation model. Further support of this model has come from a joint observation between the FCS and H-alpha spectra taken from the ground (Acton et al. 1982). They have taken the output from a comprehensive MHD model comparing the observed H-alpha profiles to those predicted to be a signature of the evaporation process and found good qualitative agreement. Also the amount of material that was calculated to be taking part in this process would be sufficient to

supply the material seen later in the corona. Further work on mass motions in flares has been done by Bentley et al. who have discovered high velocity (300-400 km/s) flows in the high temperature plasma ($>10^7$ K) of a limb flare where such Doppler motion have not been expected to be observed. This event was associated with a coronal transient.

With the BCS it is possible to follow the evolution of flare parameters such as temperature and emission measure with good time resolution, at least for the higher temperature component of the coronal plasma. The FCS can produce the temperature distribution of the differential emission measure (DEM) over the 2-70 million K temperature range but with a lower sampling rate. This has been done for a number of flares, and we find that it produces a two-component model with each being comparable energetically. This, in conjunction with other SMM instruments, can yield a complete energy budget for the coronal portion of a flare (see Figure 4). The FCS also can supply the time history of several components of the coronal plasma when used in its wavelength scanning mode. Figure 5 shows the evolution of the flare density throughout a double flare on 5 November 1980, from a paper by Wolfson et al 1983.

P. Bornmann has found that the shape of the light curves of the HP lines can give an indication of the temperature of the coronal plasma; she observed changes of slope in the light curves of these lines as the coronal plasma cooled through its peak formation temperature. This work is still under way and will be a major part of her thesis. An important discovery of SMM-I was that of large coronal arches filled with hot plasma several hours after the onset of a two ribbon flare. While the HXIS instrument was the primary one to image these structures (see Svestka et al. 1982) the BCS was able to support this analysis by supplying observations of the temperature and emission measure of the plasma from long integration spectra.

The XRP experiment has often been used in support of radio observations from ground sites all over the world. An example of this

study was the discovery that there may be some association between Long Duration Events and Type I metric noise storms (Lantos et al. 1981). Using a combination of FCS and BCS data we found that the storm is located in the leg of a loop transient, and that the production of the metric burst, the white light transient and the extended emission of soft X-rays are closely linked.

One of the potentially most interesting results from the XRP experiment is the discovery of indications that the heavy element abundances in flares may be varying by as much as 40%. This result (Sylwester, Mewe and Lemen, 1984) comes from ratios of the Ca XIX resonance line intensity to that of the nearby thermal continuum. The ratio, when plotted as a function of temperature (Figure 6), often shows some hysteresis. There is also variation in this ratio from flare to flare. This could be very important in the interpretation of flare spectra in the future.

4.2. Active Region Observations and Results

The FCS has compiled an unprecedented record of the complete transit of several large active regions across the solar disk. In both the 1980 and 1984 operational periods the FCS followed the complete evolution of the soft X-ray emission of active regions from emergence until their decay or passage over the limb. With images taken on time scales of between 2 and 30 minutes throughout its transit, we have data sets that will be invaluable in following the relationship between the state of the photospheric magnetic field (from ground-based magnetographs) and the soft X-ray output of the region. This is particularly important in relation to flare production. These data have been the subject of several FBS and SERF workshops and related publications. Figure 7 shows several stages in the transit of NOAA Active Region 4492/4.

We have made several joint observations of active region loop arcades with microwave radio instruments (particularly the VLA). In some work by Schmahl et al. 1982 we were able to derive estimates of the coronal

magnetic fields by combining microwave, optical and X-ray images of an active region. Further, we have been able to shed some light on the emission mechamism that causes microwave "rings" around sunspots.

The FCS produced a very interesting result from some early soft X-ray line profiles taken in a limb active region. These data showed that the resonance lines of O VIII, Ne IX and Mg XI were broader than the instrument profile. This could not be explained satisfactorily by simple thermal effects and so was attributed to Doppler motions (namely turbulence) by Acton et al. 1981. This work has been followed up in the 1984 operations period. Initial results confirm the earlier result, giving a turbulent velocity in quiescent active region loops of about 100 km/s and an upper limit to any flows of about 20 km/s. Figure 8 shows the spatial distribution of Mg XI line profiles obtained by the FCS. This work brings into doubt the validity of static loop models that have been relied on for a number of years. We have also made observations of the He-like triplet lines, which should give us at least a lower limit on the densities in coronal active region loops.

4.3 Quiet Sun Observations and Results

The XRP was not designed to look at the quiet Sun but with sufficient integration time and a stable structure it has been shown that the FCS can detect quiet Sun sources and get data that can be useful in limiting some of the physical quantities involved. As we have been developing better background subtraction techniques, such studies have become more feasible. The first attempt at this was in a study of Ephemeral Active Regions (EAR), or coronal bright points, by Tang et al. 1983 who combined ground-based observations with those from SMM to look at the nature of the phenomenon. We have also detected X-ray signals from bright spotless plages and active filaments (and prominences). A recent attempt has been made to look at the Doppler motions across a coronal hole boundary by using the FCS, but the data have not yet been fully reduced and so there are no definitive results from that study at present.

4.4 Atomic Physics Results

Comparisons of synthetic spectra derived from atomic models with our data have led to significant improvements in the models. This is particularly the case for the Ca XIX spectrum observed by the BCS; E. Antonnucci and J. Dubois have improved the agreement between the model and the observed Ca XIX and Fe XXV spectra since the start of the SMM (see Figure 9 for an example of a synthetic spectral fit to BCS data). Note that the intercombination lines are not fit well as yet. This will be a subject of future studies.

Work by Phillips et al. 1984 on the inner shell transitions of Fe XIX to Fe XXII has compared the results from calculated spectra to those from both tokamaks and from coronal plasma observed by the BCS. It was found that the density dependence of the Fe XX lines was confirmed and could be a useful diagnostic for certain high density cosmic X-ray sources such as Sco X1.

The BCS also observes the K-alpha transition of iron (1.94 A); there was some speculation as to the true formation mechanism of this line. In a paper by Parmar et al. 1984 it is established that the prime source is due to photospheric fluorescence from hard X-rays in the corona. The alternative model, a high-energy electron impact, would not have produced the observed center to limb variation in the relative output of Fe K-alpha or its timing with respect to the hard X-ray burst.

The FCS obtained a complete spectrum over its full wavelength range on 25 August 1980; these spectra enabled us to identify several hundred lines and find a few previously unknown lines (see Phillips et al. 1982). We also obtained some interesting Fe XVII line ratios since the SMRM, which indicate that there remains some work to be done in understanding that ion.

4.5 Absolute Flux Calibration of the FCS

Many XRP science results depend critically upon the knowledge of the relative and absolute flux calibration of the individual FCS channels: i.e., the O/Ne abundance ratio, temperature-dependent line ratios from different channels, home-position x-ray light curves using sit-and-stare data, and the use of FCS absolute line fluxes in conjunction with results from other SMM experiments. Hence some substantial effort has gone into understanding the overall FCS calibration, focusing on two areas in particular: 1) the "pedestal problem" and 2) the thin window detector calibration (#s 1 and 2).

The FCS "pedestal" is a spurious contribution to the detector counting rates thought to be largely the result of x-ray fluourescence of the FCS (and BCS!) crystals in response to harder x-ray photons during a flare. The initial pedestal correction was found to be inaccurate for large flares, and a new analysis of the problem was performed by R. Stern. This resulted in a new pedestal correction algorithm, which K. Strong and R. Stern have tested against sit-and-stare data from the 14 Oct 1980 flare; they find it to be in general a much better behaved algorithm than that previously used. The pedestal correction in some cases can be as much as 50% of the total count rate in some channels, and therefore substantially changes derived line ratios in different home position lines.

Because the O/Ne abundance in flares is a scientifically important abundance ratio, and because the O VIII and Ne IX resonance lines are at the home positions of channels 1 and 2, the relative calibration of these two channels is highly relevant to such abundance studies. A cross-calibration of the two detectors was performed after the SMM repair by scanning the Ne IX triplet in both detectors 1 and 2, indicating agreement to within ~ 30%. However, The calibration of detector #1 at the O VIII resonance line (18.97 A) is much more dependent upon accurate window thickness measurements than the results at Ne IX (13.45 A). A reanalysis of the original window calibration data by R. Stern suggested that the detector 1 window was, in fact,

about 10% thicker than was assumed in the original FCS sensitivity calculations by Leibacher and Rapley, reducing a long-standing discrepancy in the O/Ne abundance ratio by a factor of 1.5. Further work is currently being done to calibrate the effect of detector gain performance on the Channel 1/Channel 2 relative sensitvity. A direct consequence of this work will also be a better absolute flux calibration of the two detectors.

5. Acknowledgements

Construction and operation of an instrument of this complexity has depended on the commitment and efforts of a substantial team over a period of a decade. We acknowledge with sincere thanks the contributions of colleagues, sub-contractors, suppliers, and especially the agencies and individuals sponsoring the research program. The two British groups have been supported by the UK Science and Engineering Research Council. The Lockheed program has been supported by the National Aeronautiucs and Space Administration through the Goddard Space Flight Center.

The Appleton Laboratory team responsible for the FCS structure and mechanisms included B. A. Barker, J. E. Pateman, D. C. Tredgett, A. Wilson, R. F. Turner and J. Firth. W. G. Griffin was responsible for alignment of the FCS system and B. E. Patchett contributed to the evaluation of FCS optical systems.

The Mullard Space Science Laboratory team responsible for the mechanical desing and construction of the BCS and FCS gas system and detectors included W. Gilford, J. Coker, R. Dryden and C. Dela Nougerade. Those responsible for electronic design, testing and construction work on BCS and FCS pulse processing and gas control circuitry included M. Day, D. Hoyle and J. Ootes. In addition we are grateful to Bob Nettleship and his colleagues at Pye Telecommunications for supplying several of the electronic subsytems for both instruments. Major parts of the X-ray detector construction were undertaken by John Leake and his associates at the UK Atomic Energy

Research Establishment at Harwell and we are especially grateful to them for their skilled and dedicated work.

The Lockheed team responsible for the FCS collimator included T. Miller, Ruth Peterson, S. W. Salat, R. J. Salmon and J. R. Vieira. T. Pope was primarily responsible for the FCS alignment sensor. A. M. Cosner and S. R. Keith are acknowledged for their contributions to design of XRP software, and B. C. Rix for his work on ground support equipment. Richard Deslattes, A. R. Burek and colleagues at the National Bureau of Standards provided invaluable counsel and assistance on all matters dealing with crystals.

For support of mission operations we acknowledge the Grumman operating team under the direction of J. Harrison. Technical support for planning of solar observations was provided by D. Speich and J. Nelson and their colleagues at NOAA. We acknowledge the efficient work of the NASA SMM project team, initially under P. Burr and J. Donley, more recently headed by P. Corrigan, in carrying out the SMM observations. Other scientific and technical support has come from M. Kayat, R. D. Bentley, J. A. Bowles, M. L. Finch, C. W. Gilbreth, P. Guttridge, R. W. Hayes, E. G. Joki, B. B. Jones, B. J. Kent, J. W. Leibacher, R. A. Nobles, T. J. Patrick, K. J. H. Phillips, C. G. Rapley, P. H. Sheather, J. C. Sherman, J. P. Stark, L. A. Springer, and R. F. Turner.

Lastly, we wish to acknowledge our two British colleagues and co-Principal Investigators, Dr. J. L. Culhane and Dr. Alan H. Gabriel, whose enthusiasm and leadership made this mission possible.

FIGURE 1: Spectral coverage of the seven FCS channels with some important X-ray lines indicated. Any vertical line will indicate a polychromatic position of the spectrometer. The "home position" lines are indicated by the arrow.

FIGURE 2: Spectral coverage of the eight BCS channels showing observation of a bright flare on 1 July 1980.

FIGURE 3: Two Ca XIX Spectra from an X-13 flare that occurred on 24 April 1984. The lower spectrum was taken during onset of the flare burst and shows considerable line broadening and line shifts, which we attribute to Doppler motions of several hundred km/s. The upper spectrum shows the decay phase of the flare; note that the lines are narrower and no longer shifted and that the satellite lines are now clearly seen.

FIGURE 4: Various measureable energy components of the 8 April 1980 flare, showing the energy budget as a function of time for this event.

FIGURE 5: Temporal variation of the Ne IX resonance line emission, the G and R ratios, and the resultant electron density for the large solar flare of 5 November 1980.

FIGURE 6: The line to continuum ratio plotted against temperature for the cooling phases of two flares. The mean electron temperature has been estimated from the satellite to resonance line ratios. The constant vertical shift between the two flares corresponds to a variation in the Ca abundance by a factor of ~ 1.4.

FIGURE 7: A time series of five FCS images in three of the soft X-ray channels corresponding to ~ 2-5 million K emission, along with the FCS white light image showing where the X-rays originate with respect to the photosphere. These were taken on five successive days as AR 4492/4 moved across the solar disk.

FIGURE 8: A series of line profiles from the FCS, each at a different point in AR 4474 in April 1984. This shows variations in line widths from pixel to pixel indicating mass motions in the quiescent region.

FIGURE 9: A BCS Ca XIX spectrum taken during the 14 July 1980 flare compared to the predictions of a theoretical model by Dubois et al. Note the goodness of the fit, except for satellite lines x and y; this is still being studied.

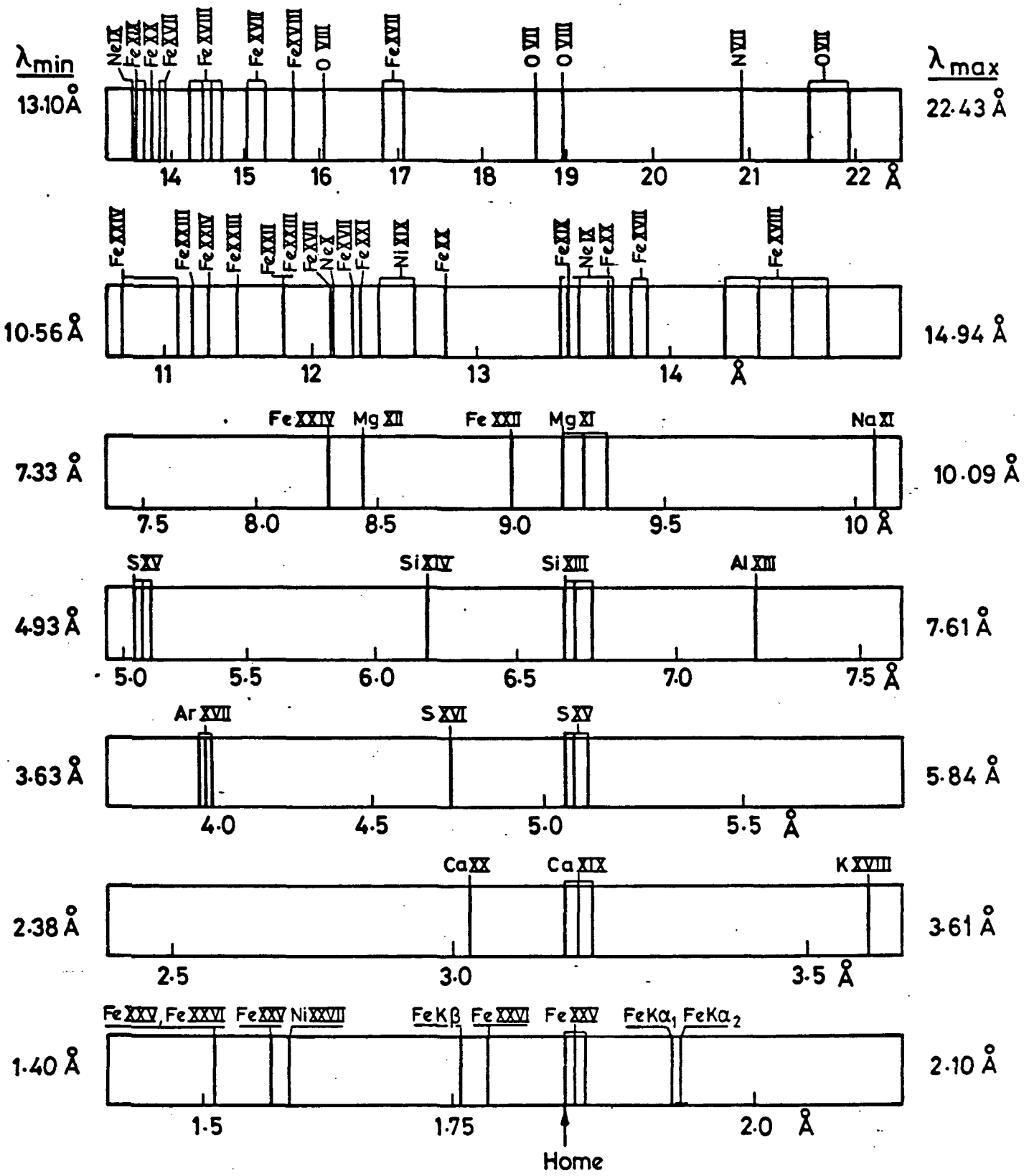
λmin
13.10Å
λmax
22.43 Å
Ne IX
Fe XIII
Fe XX
Fe XVII
Fe XVIII
Fe XVII
Fe XVIII
O VIII
Fe XVII
O VIII
O VIII
N VII
O VIII
14 15 16 17 18 19 20 21 22 Å
Fe XXIV
Fe XXIII
Fe XXIV
Fe XXIII
Fe XXIII
Fe XXIII
Fe XVII
Ne X
Fe XVII
Fe XXI
Ni XIX
Fe XX
Fe XIX
Ne IX
Fe XX
Fe XVII
Fe XVIII
10.56 Å
14.94 Å
11 12 13 14 Å
Fe XXIV
Mg XII
Fe XXII
Mg XI
Na XI
7.33 Å
10.09 Å
7.5 8.0 8.5 9.0 9.5 10 Å
S XV
Si XIV
Si XIII
Al XIII
4.93 Å
7.61 Å
5.0 5.5 6.0 6.5 7.0 7.5 Å
Ar XVII
S XVI
S XV
3.63 Å
5.84 Å
4.0 4.5 5.0 5.5 Å
Ca XX
Ca XIX
K XVIII
2.38 Å
3.61 Å
2.5 3.0 3.5 Å
Fe XXV, Fe XXVI
Fe XXV
Ni XXVII
FeKβ
Fe XXVI
Fe XXV
FeKα1
FeKα2
1.40 Å
2.10 Å
1.5 1.75 2.0 Å
Home

FIGURE 1

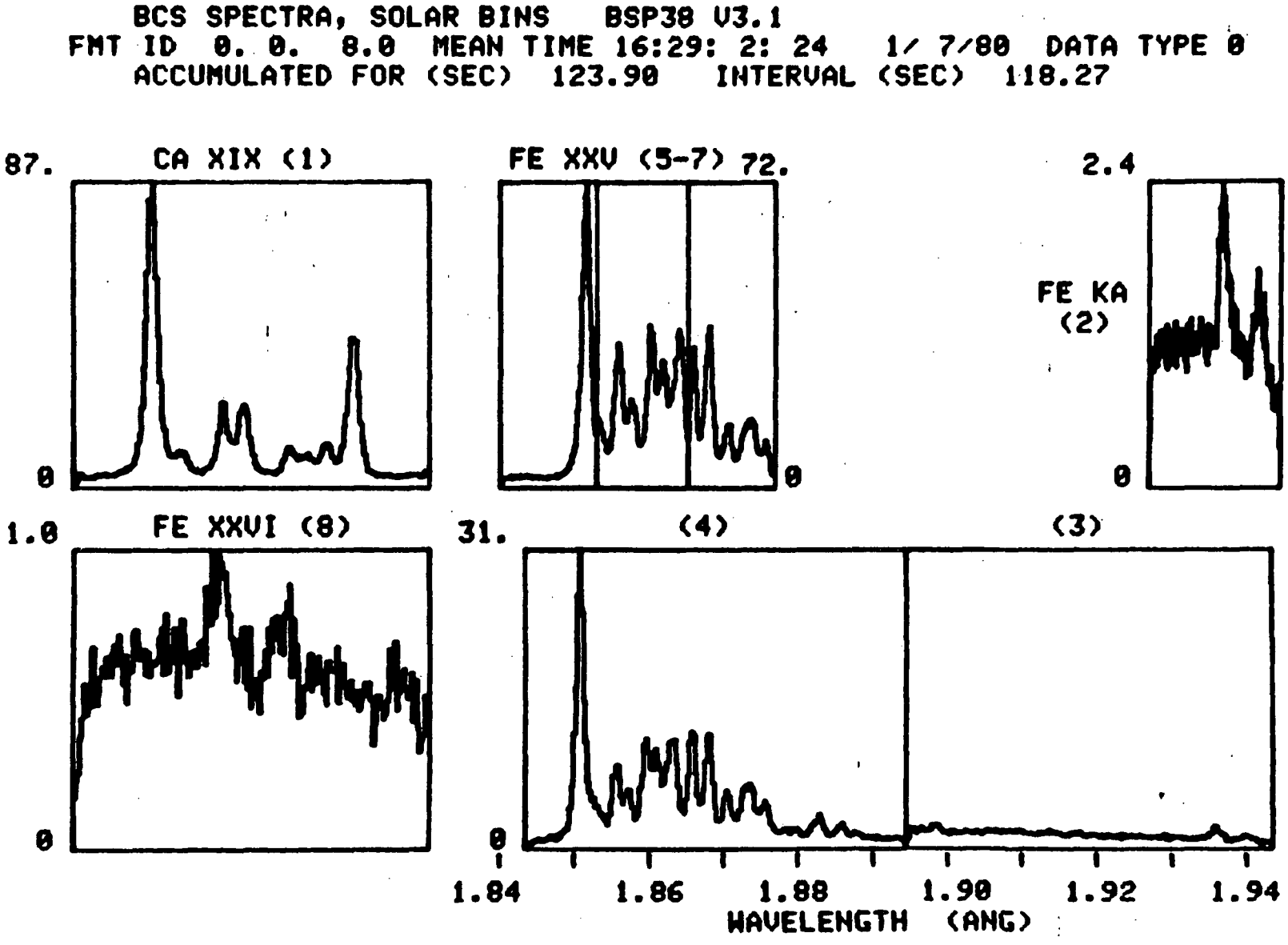
BCS SPECTRA, SOLAR BINS BSP38 V3.1
FMT ID 0. 0. 8.0 MEAN TIME 16:29: 2: 24 1/ 7/80 DATA TYPE 0
ACCUMULATED FOR (SEC) 123.90 INTERVAL (SEC) 118.27
87.
CA XIX (1)
0
FE XXV (5-7) 72.
0
2.4
FE KA
(2)
0
1.0
FE XXVI (8)
0
31.
(4)
(3)
0
1.84
1.86
1.88
1.90
1.92
1.94
WAVELENGTH (ANG)

FIGURE 2

BCS CA XIX SPECTRA DURING X13 FLARE

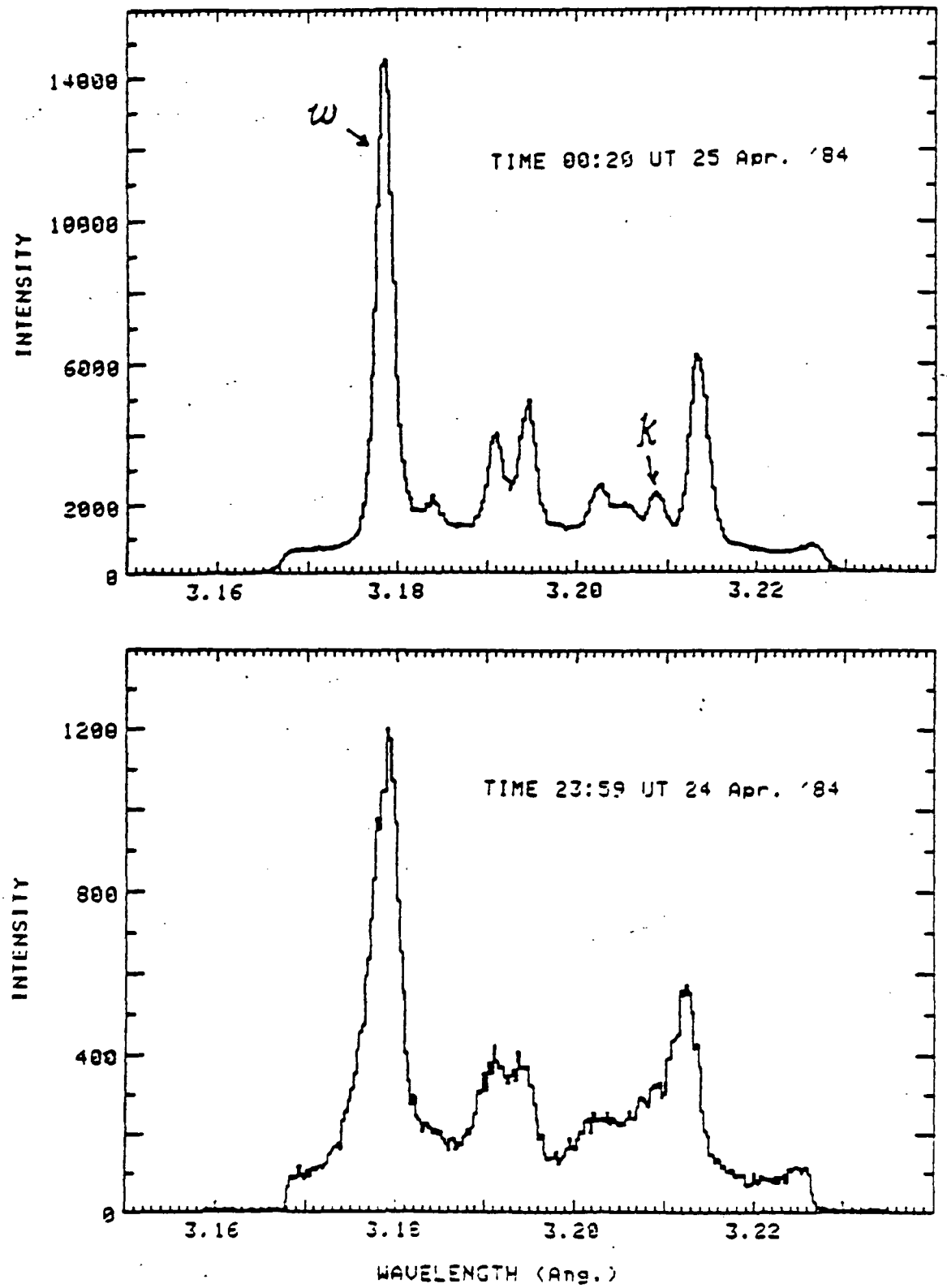

FIGURE 3

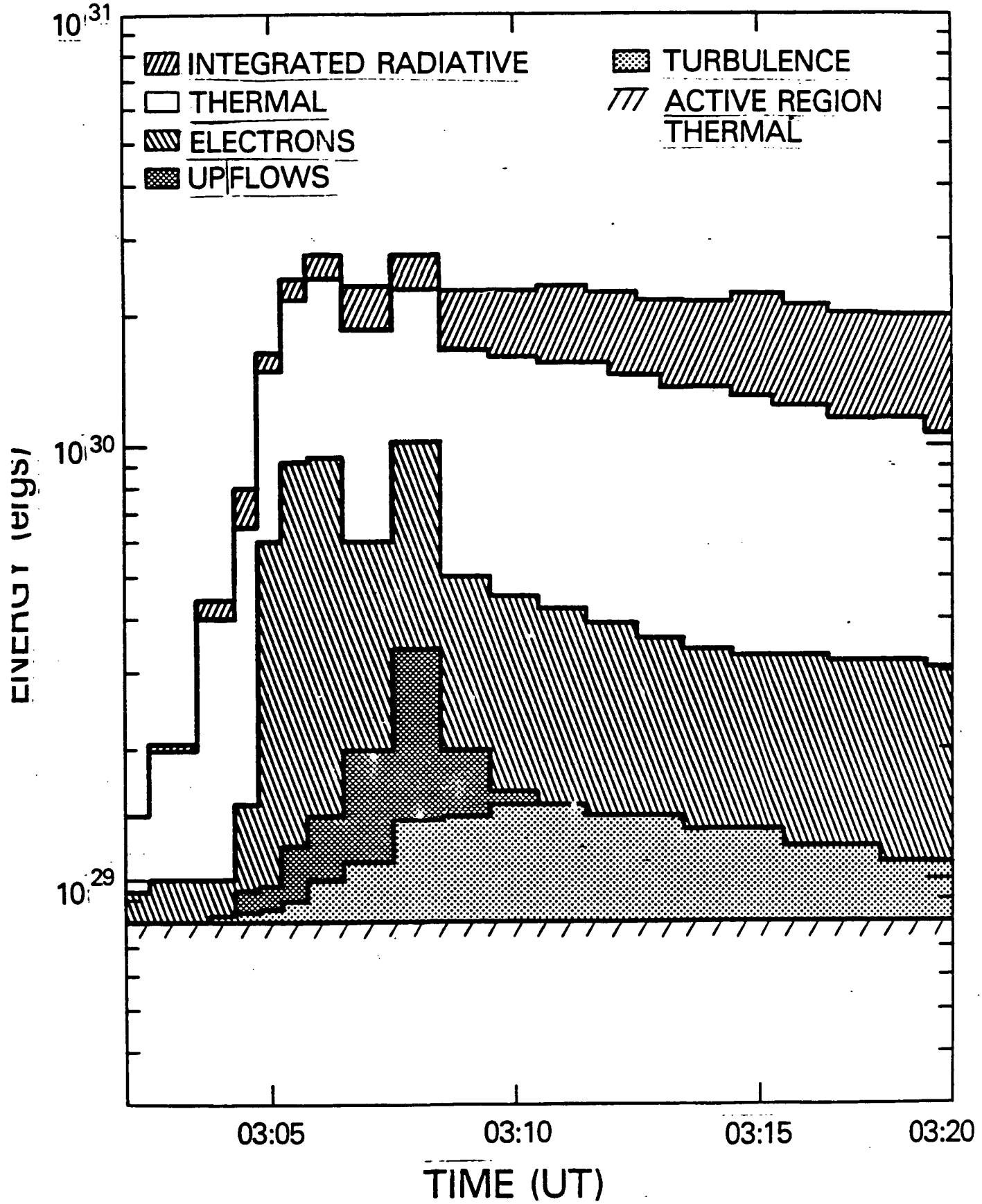
INTEGRATED RADIATIVE
THERMAL
ELECTRONS
UP FLOWS
TURBULENCE
ACTIVE REGION THERMAL
10^{31}
10^{30}
10^{29}
ENERGY (ergs)
03:05
03:10
03:15
03:20
TIME (UT)

FIGURE 4

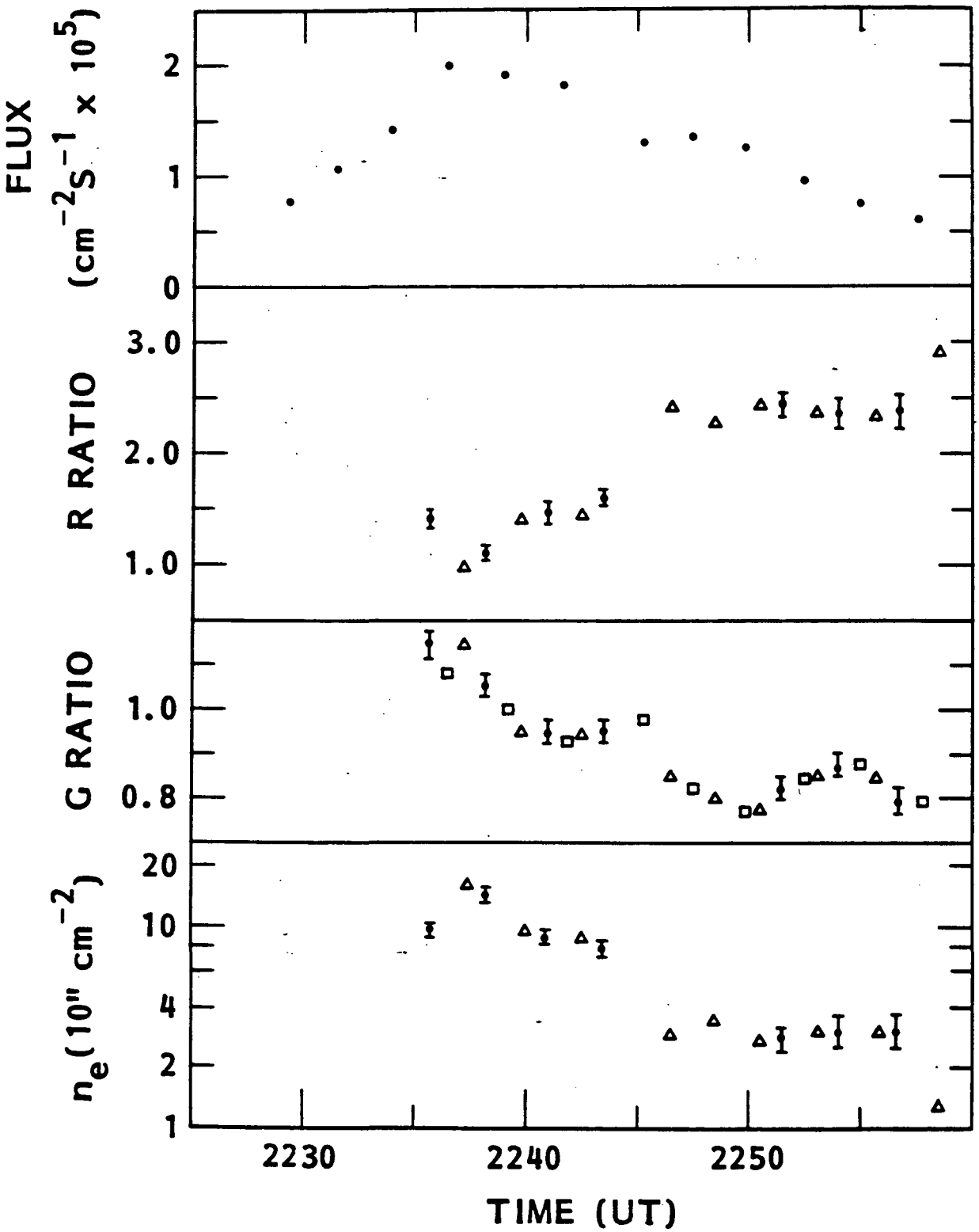
FLUX
(cm^{-2}S^{-1} x 10^5)
2
1
0
R RATIO
3.0
2.0
1.0
G RATIO
1.0
0.8
n_e(10" cm^{-2})
20
10
4
2
1
2230
2240
2250
TIME (UT)

FIGURE 5

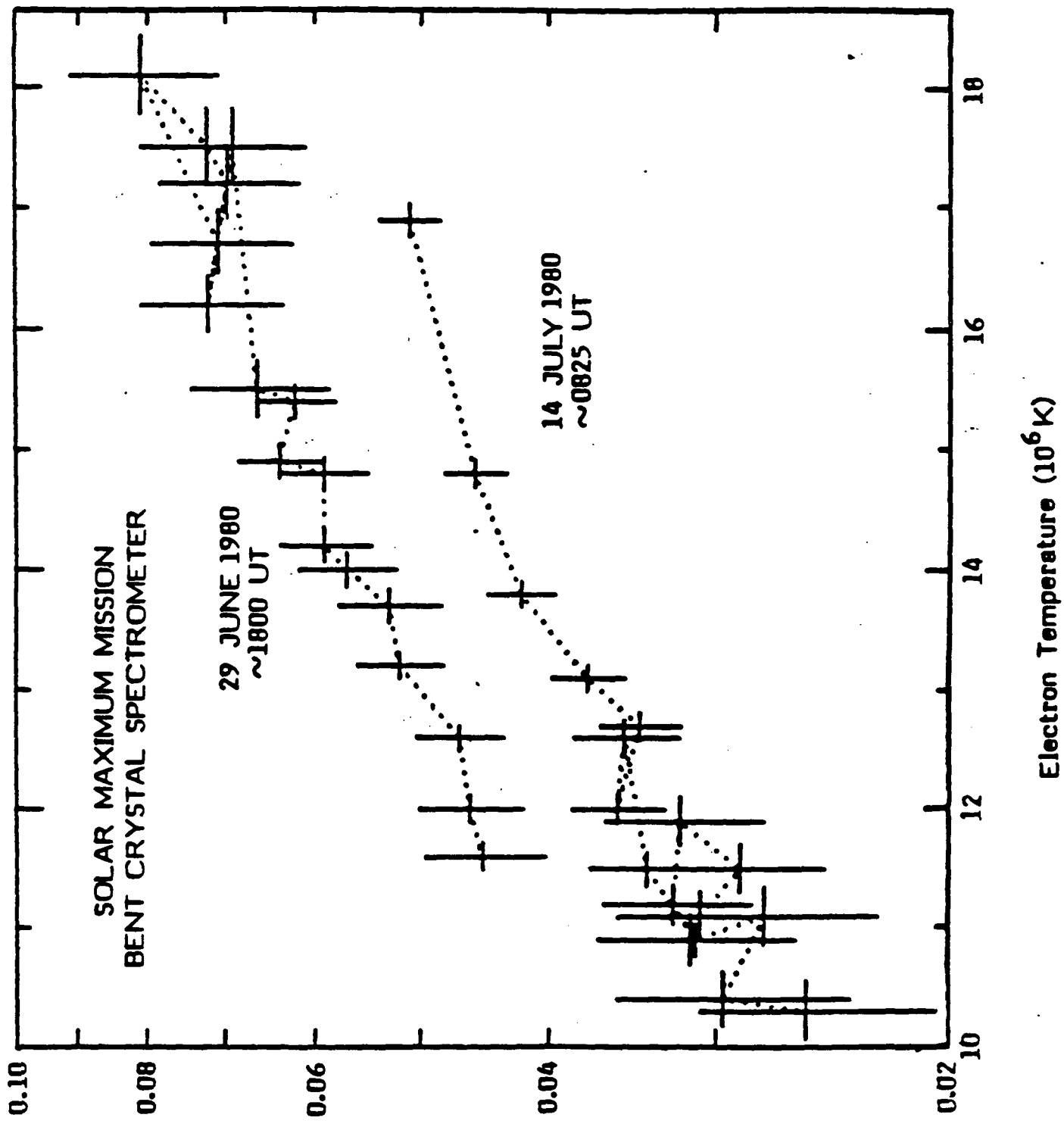
SOLAR MAXIMUM MISSION
BENT CRYSTAL SPECTROMETER
29 JUNE 1980
~1800 UT
14 JULY 1980
~0825 UT
Line to Continuum Ratio (Å^{-1})
Electron Temperature (10^6K)
0.10
0.08
0.06
0.04
0.02
10
12
14
16
18

FIGURE 6

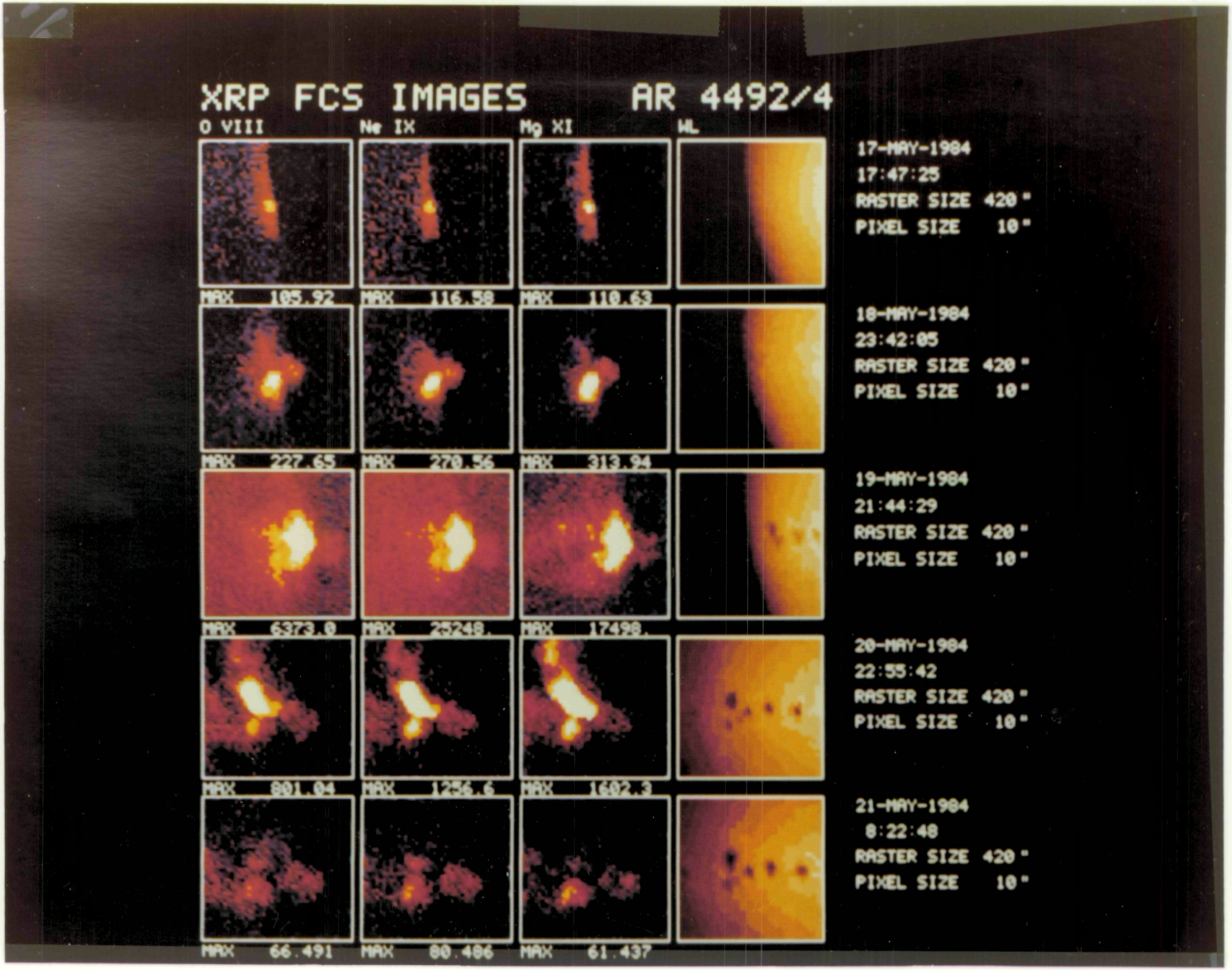
XRP FCS IMAGES AR 4492/4
O VIII
Ne IX
Mg XI
WL
17-MAY-1984
17:47:25
RASTER SIZE 420"
PIXEL SIZE 10"
MAX 105.92
MAX 116.58
MAX 110.63
18-MAY-1984
23:42:05
RASTER SIZE 420"
PIXEL SIZE 10"
MAX 227.65
MAX 270.56
MAX 313.94
19-MAY-1984
21:44:29
RASTER SIZE 420"
PIXEL SIZE 10"
MAX 6373.0
MAX 25248.
MAX 17498.
20-MAY-1984
22:55:42
RASTER SIZE 420"
PIXEL SIZE 10"
MAX 801.04
MAX 1256.6
MAX 1602.3
21-MAY-1984
8:22:48
RASTER SIZE 420"
PIXEL SIZE 10"
MAX 66.491
MAX 80.486
MAX 61.437

FIGURE 7

FOS Spectroscopic Scan in a Raster

MG XI Home Position Profile

2' X 1' Raster with 15" Pixels

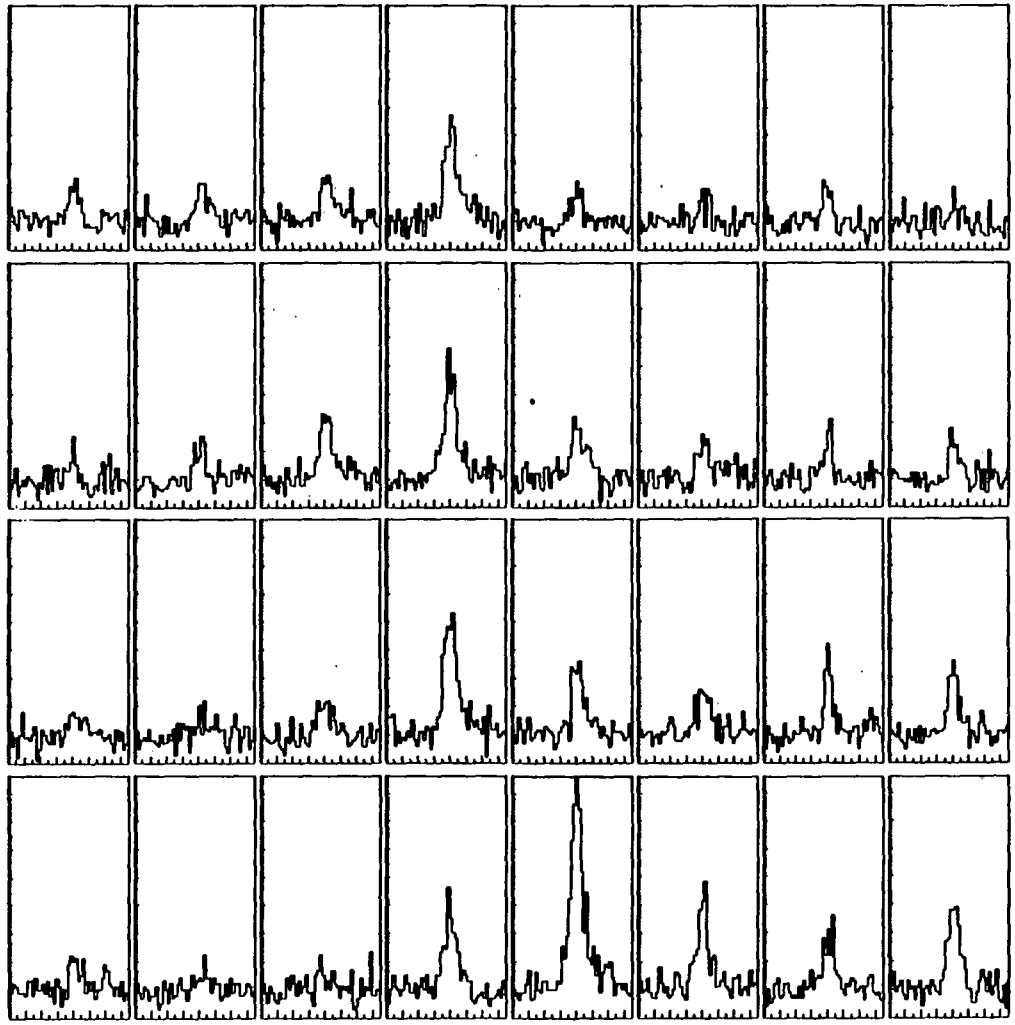

N

W

Intensity

Wavelength Range: 9.15 – 9.19 A

FIGURE 8

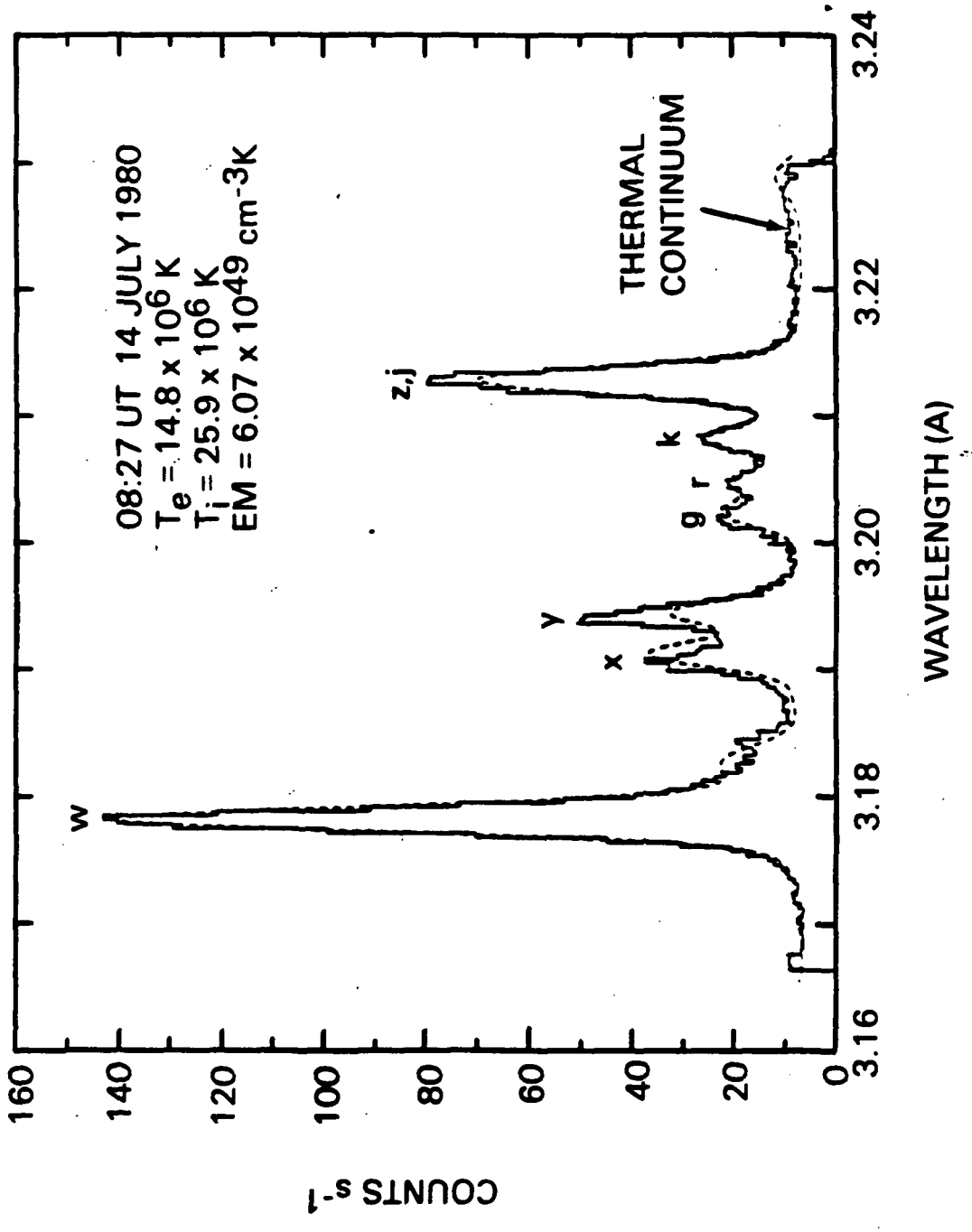
BCS Ca XVIII — XIX
08:27 UT 14 JULY 1980
T_e = 14.8 x 10^6 K
T_i = 25.9 x 10^6 K
EM = 6.07 x 10^{49} cm^{-3}K
w
x
y
z,j
q
r
k
THERMAL CONTINUUM
COUNTS s^{-1}
WAVELENGTH (A)
0
20
40
60
80
100
120
140
160
3.16
3.18
3.20
3.22
3.24

FIGURE 9

APPENDIX A: XRP BIBLIOGRAPHY

I. PUBLISHED PAPERS

1979

An Analysis of the XRP Raster Mechanism: D.M. Simpson, Appleton Laboratory, Report AL-R-6, June 1979.

1980

The Soft X-Ray Polychromator for the Solar Maximum Mission: L.W. Acton, J.L. Culhane, A.H. Gabriel, R.D. Bentley, J.A. Bowles, J.G. Firth, M.L. Finch, C.W. Gilbreth, P. Guttridge, R.W. Hayes, E.G. Joki, B.B. Jones, B.J. Kent, J.W. Leibacher, R.A. Nobles, T.J. Patrick, K.J.H. Phillips, C.G. Rapley, P.H. Sheather, J.C. Sherman, J.P. Stark, L.A. Springer, R.F. Turner, and C.J. Wolfson, Sol. Phys. 65, 53-71, 1980.

Large-aperture High-Resolution X-Ray Collimator for the Solar Maximum Mission: R.A. Nobles, L.W. Acton, E.G. Joki, J.W. Leibacher and R.C. Peterson, Appl. Opt., 19, 2957, 1980.

Multithermal Analysis of Solar X-Ray Line Emission: J. Sylwester, J. Schrijver and R. Mewe, Sol. Phys., 67, 285-309, 1980.

1981

Dielectronic Satellite Spectra for Hydrogen-Like Iron in Low Density Plasmas: J. Dubau, A.H. Gabriel, M. Loulergue, L. Steenman-Clark and S. Volonte, Mon. Not. R. astr. Soc., 195, 705-719, 1981.

Observations of Transitions of Hydrogen-Like Fe XXVI in Solar Flare Spectra: A.N. Parmar, J.L. Culhane, C.G. Rapley, E. Antonucci, A.H. Gabriel and M. Loulergue, Mon. Not. R. astr. Soc., 197, 29P-34P, 1981.

Dielectronic Satellite Spectra for High Charged Helium-Like Ions - VI. Iron Spectra with Improved Inner-Shell and Helium-Like Excitation Rates: F. Bely-Dubau, J. Dubau, P. Faucher and A.H. Gabriel, Mon. Not. R. Astr. Soc., 198, 239-254, 1981.

Classification of the Spectra of Highly Ionized Atoms during the Last 7 Year: B.C. Fawcett, Physica Scr., 24, no. 4, 663-680, 1981.

Solar Flare Plasmas: A.H. Gabriel, Phil. Trans. R. Soc. Lond., A300, 497, 1981.

The Surface Preparation of Beryl Crystals for X-Ray Spectroscopy: R.W. Hayes and B.J. Kent, J. Phys. E: Sci. Instr., 14, 689, 1981.

Early Results from the Soft X-Ray Polychromator Experiment: A.H. Gabriel, J.L. Culhane, L.W. Acton, E. Antonucci, R.D. Bentley, C. Jordan, J.W. Leibacher, A.N. Parmar, K.J.H. Phillips, C.G. Rapley, C.J. Wolfson and K.T. Strong, J. Space Res. 1, 267, 1981.

X-Ray Line Width and Coronal Heating: L.W. Acton, J.L. Culhane, A.H. Gabriel, C.J. Wolfson, C.G. Rapley, K.J.H. Phillips, E. Antonucci, R.D. Bentley, R.W. Hayes, E.G. Joki, C. Jordan, M. Kayat, B. Kent, J.W. Leibacher, R.A. Nobles, A.N. Parmar, K.T. Strong and N.J. Veck, Astrophys. J. 244, L137-L140, 1981.

X-Ray Spectra of Solar Flares Obtained with a High Resolution Bent Crystal Spectrometer: J.L. Culhane, A.H. Gabriel, L.W. Acton, C.G. Rapley, K.J.H. Phillips, C.J. Wolfson, E. Antonucci, R.D. Bentley, R.C. Catura, C. Jordan, M. Kayat, J.W. Leibacher, P. McWhirter, A.N. Parmar, J. Sherman, L. Springer, K.T. Strong and N.J. Veck, Astrophys. J. (Letters), 244, L141-L151, 1981.

Observations of the Limb Solar Flare on 1980 April 30 with the SMM X-Ray Polychromator: A.H. Gabriel, L.W. Acton, J.L. Culhane, K.J.H. Phillips, C.J. Wolfson, C.G. Rapley, E. Antonucci, R.D. Bentley, C. Jordan, M. Kayat, J.W. Leibacher, M. Levay, J. Sherman, K.T. Strong and N.J. Veck, Astrophys. J. (Letters), 244, L147, 1981.

Relationship Between a Soft X-Ray Long Duration Event and an Intense Metric Noise Storm: P. Lantos et al., Astron. Astrophys., 101, 33-38, 1981.

Simultaneous Radio Optical and Space Observation of AR 2490: F. Chiuderi-Drago, Proceedings of International Workshop on Solar Maximum Year, Moscow, IZMIRAN, , 1, 1981.

1982

Solar Observations Using the Soft X-Ray Polychromator Experiment on SMM: E. Antonucci, C.J. Wolfson, C.G. Rapley, L.W. Acton, J.L. Culhane, A.H. Gabriel; Proceedings of International Workshop on Solar Maximum Year, Simferopol, Moscow, IZMIRAN V, 1, 62, 1982.

Observations of a Post-Flare Radio Burst in X-Rays: Z. Svestka, R.T. Stewart, P. Hoyng, W. Van Tend, L.W. Acton, A.H. Gabriel, C.G. Rapley, A. Boelee, E.C. Bruner, C. de Jager, H. Lafleur, G. Nelson, G.M. Simnett, H.F. Van Beek and W.J. Wagner, Sol. Phys., 75, 305-329, 1982.

Observation of Solar Flare Transition-Zone Plasmas from the Solar Maximum Mission: C-C. Cheng, E.C. Bruner, E. Tandberg-Hanssen, B.E. Woodgate, R.A. Shine, P.J. Kenny, W. Henze and G. Poletto, Astrophys. J., 253, 353, 1982.

Transition Region Oscillations in Sunspots: J. Gurman, J.W. Leibacher, R.H. Shine, B.E. Woodgate and W.E. Henze, Astrophys. J., 253, 939-948, 1982.

Solar Flare X-Ray Spectra from the SMM Flat Crystal Spectrometer: K.J.H. Phillips, J.W. Leibacher, C.J. Wolfson, J.H. Parkinson, B. Fawcett, B. Kent, H. Mason, L.W. Acton, J.L. Culhane and A.H. Gabriel, Astrophys. J., 256, 774-787, 1982.

Impulsive Phase of Flares in Soft X-Ray Emission: E. Antonucci, A.H. Gabriel, L.W. Acton, J.L. Culhane, C.J. Doyle, J.W. Leibacher, M. Machado, L.E. Orwig and C.G. Rapley, Sol. Phys., 78, Vol. 1, 107-124, 1982.

Comparison of Observed Ca XIX and Ca XVII Relative Line Intensities With Current Theory: C. Jordan and N.J. Veck, Sol. Phys., 78, 125-140, 1982.

The Impulsive and Gradual Phases of a Solar Limb Flare as Observed from the Solar Maximum Mission Satellite: A.I. Poland, M.E. Machado, C.J. Wolfson, K.J. Frost, B.E. Woodgate, R.A. Shine, P.J. Kenny, C.C. Cheng, E.A. Tandberg-Hanssen, E.C. Bruner and W. Henze, Sol. Phys., 78, 2, 201, 1982.

Multiple Wavelength Observations of a Solar Active Region: F. Chiuderi-Drago, R. Bandiera, F. Falciani, E. Antonucci, K.R. Lang, R.F. Willson, K. Shibaski and C. Slottje, Sol. Phys., 80, 71-85, 1982.

Soft X-Ray Descriminators of Flare Classification: E. Antonucci, The Observatory, 102, 121-122, August 1982.

Flare Classification - Fact or Fancy: L.W. Acton, The Observatory, 102, 1049, 123-124, August 1982.

Unusual Coronal Activity Following the Flare of 6 November 1980: Z. Svestka, B.R. Dennis, M. Pick, A. Raoult, C.G. Rapley, R.T. Stewart and B.E. Woodgate, Sol. Phys., 80, 143-159, 1982.

Active Region Magnetic Fields Inferred from Simultaneous VLA Microwave Maps, X-Ray Spectroheliograms and Magnetograms: E. Schmahl, M. Kundu, K.T. Strong, R.D. Bentley, J.B. Smith, Jr., and K. Krall, Sol. Phys., 80, 233, 1982.

Raies Satellites de Recombinaison Dielectronique: J. Dubau and S. Volonte, Ann. Phys. Fr., 7, 455-464, 1982.

Direct Evidence for Chromospheric Evaporation in a Well-Observed Compact Flare: L.W. Acton, R.C. Canfield, T.A. Gunkler, H.S. Hudson, A.L. Kiplinger and J.W. Leibacher, Astrophys. J., 263, 409-422, 1982.

Dielectronic Satellite Spectra for Highly-Charged Helium-Like Ions. VI. Iron Spectra with Improved Inner-shell and Helium-like Excitation Rates: F. Bely-Dubau, J. Dubau, P. Faucher, and A.H. Gabriel, Mon. Not. R. astr. Soc., 198, 239-254, 1982.

Dielectronic Satellite Spectra for Highly-Charged Helium-Like Ions. VII. Calcium Spectra - Theory and Comparison with SMM Observations: F. Bely-Dubau, J. Dubau, P. Faucher, A.H. Gabriel, M. Loulergue, L. Steenman-Clark, S. Volonte, E. Antonucci and C.G. Rapley; Mon. Not. R. astr. Soc., 201, 1155, 1982.

Chromospheric Evaporation Observed in Soft X-Ray Flares: E. Antonucci, Mem. della Soc. Astron. Ital., 53(2), 495-509, 1982.

Solar Physics. Chapter 10 in Applied Atomic Collision Physics, Vol. 1: A.H. Gabriel and H.E. Mason, (ed. Massey and Bates, Academic Press 1982).

1983

The Queens' Flare: Its Structure and Development; Precursors, Pre-Flare Brightenings, and Aftermaths: C. de Jager, M.E. Machado, A. Schadee, K.T. Strong, Z. Svestka, B.E. Woodgate and W. van Tend, Sol. Phys., 84, 205-236, 1983.

Inner Shell Transitions in Fe XIX-XXII in X-Ray Spectra of Solar Flares and Tokamaks: K.J.H. Phillips, J.R. Lemen, R.D. Cowan, G.A. Doschek and J.W. Leibacher, Astrophys. J., 265, 1120-1134, 1983.

X-Ray Line Ratios from He-Like Ions: Updated Theory and SMM Flare Observa- tions: C.J. Wolfson, J.G. Doyle, J.W. Leibacher, and K.J.H. Phillips, Astrophys. J., 269, 319-328, 1983.

Closed Coronal Structures V. Gas-dynamic Models of Flaring Loops and Comparison with SMM Observations: R. Pallavicini, G. Peres, S. Serio, G. Vaiana, L.W. Acton, J.W. Leibacher and R. Rosner, Astrophys. J., 270, 270-287, 1982.

Non-Thermal and Non-Equilibrium Effects in Soft X-Ray Flare Spectra: A.H. Gabriel, E. Antonucci, and L. Steenman-Clark, Sol. Phys., 86, 59-66, 1983.

Observations of Chromospheric Evaporation During the Solar Maximum Mission: E. Antonucci and B.R. Dennis, Sol. Phys., 86, 67-77, 1983.

Transport and Containment of Plasma, Particles and Energy within Flares: L.W. Acton, W.A. Brown, M.E.C. Bruner, B.M. Haisch and K.T. Strong, Sol. Phys., 86, 79-90, 1983.

Hydrodynamics of Flaring Loops: SMM Observations and Numerical Simulations: R. Pallavicini and G. Peres, Sol. Phys., 86, 147-156, 1983.

Microwave, Ultraviolet and Soft X-Ray Observations of Hale Region 16898: K. Shihasaki, F. Chiuderi-Drago, M. Melozzi, C. Slottje and E. Antonucci, Sol. Phys., 89, 307-321, 1983.

Bright Point Study: F. Tang, K. Harvey, M. Bruner, B.J. Kent, and E. Antonucci, Adv. Space Res., 2, 65-72, 1983.

1984

Interpretation of a Microwave Active Region Ring Structures and Other Features Using SMM Soft X-Ray Observations: K.T. Strong, C. Alissandrakis and M. Kundu, Astrophys. J., 277, 865, 1984.

A Multiwavelength Study of a Double Impulsive Flare: K.T. Strong, A.O. Benz, B.R. Dennis, J.W. Leibacher, R. Mewe, A. Poland, J. Schrivjer, G. Simnett, J.B. Smith, Jr., and J. Sylwester, Sol. Phys., 91, 325-344, 1984.

Derivation of Ionization Balance for Ca XVIII/XIX Using XRP Solar X-Ray Data: E. Antonucci, A.H. Gabriel, J.G. Doyle, J. Dubau, D. Foucher, C. Jordan and N.J. Veck., Astron. Astrophys., 133, 239-246, 1984.

Interpretation of High Resolution X-Ray Observations of Coronal Plasmas: F. Bely-Dubau, Physica Scripta, Vol T7, 34-38, 1984.

Solar Research at RAL, A.H. Gabriel, J. Brit. Interplan. Soc., 37, 317-319, 1984.

SMM Observations of K-alpha Radiation from Fluorescence of Photospheric Iron by Solar X-Rays: A.N. Parmar, C.J. Wolfson, J.L. Culhane, K.J.H. Phillips, L.W. Acton, B.R. Dennis and C.G. Rapley, Astrophys. J., 279, 866-874, 1984.

Inner-Shell Transitions of Fe XXIII and Fe XXIV in the X-ray Spectra of Solar Flares: J.R. Lemen, K.J.H. PHillips, R.D. Cowan, J. Hata and I.P. Grant, Astron. and Astrophys., 135, 313-324, 1984.

Variation in the Observed Coronal Calcium Abundance of Various X-ray Flare Plasmas: J. Sylwester, J.R. Lemen, and R. Mewe, Nature, 310, 665-666, 1984.

II. PAPERS IN PREPARATION

(a) Accepted

Magnetohydrodynamic Simulation of the Coronal Transient Associated with the Solar Limb Flare of 1980 June 29, 1821 UT: S.T. Wu, S. Wang, M. Dryer, A.I. Poland, D.G. Sime, C.J. Wolfson, L.E. Orwig and A. Maxwell, Sol. Phys., 1983.

The Development and Cooling of a Limb Flare: N.J. Veck, K.T. Strong, C. Jordan, G.M. Simnett, P.J. Cargill, and E. Priest, Mon. Not. Roy. astr. Soc., 1983.

A Consistent Picture of Coronal and Chromospheric Processes in a Well-Observed Solar Flare: T.A. Gunkler, R.C. Canfield, L.W. Acton, and A.L. Kiplinger, Astrophys. J., 1984.

The Impulsive Phase of a Limb Flare: G.M. Simnett and K.T. Strong, Astrophys. J., 1984, in press.

Progress in the study of Homologous Flares on the Sun: B.E. Woodgate, M.J. Matres, J.B. Smith, K.T. Strong, M.K. McCabe, M.E. Machado, V. Gaisauskas, R. Stewart, and P.A. Sturrock, COSPAR, Graz, Austria, Adv. in Space Res., 1984, in press.

Homologous Flares and Evolution of NOAA Active Region 2372: K.T.Strong, J.B. Smith, Jr., M. McCabe, M. Machado, J.L.R.Saba, and G.M. Simnett, COSPAR, Graz, Austria, Adv. in Space Res., 1984, in press.

Combined Analysis of Soft and Hard X-Ray Spectra from Flares: A.H. Gabriel, F. Bely-Dubau, J.C. Sherman, L.E. Orwig, H. Schrijver, COSPAR, Graz, Austria, Adv. Space Res., 1984, in press.

Origin and Location of Chromospheric Evaporation in FLares: E. Antonucci, D. Marocchi, G. M. Simnett, COSPAR, Graz, Austria, Adv. Space Res., 1984, in press.

Line Broadening and Shifts during the Impulsive Phase of Flares: E. Antonucci, Mem. della Soc. Astron. Ital., 1984, in press.

The Energetics of Chromospheric Evaporation in a Solar Flare: E. Antonucci, A.H. Gabriel and B.R. Dennis, Astrophys. J., 1984, in press.

Magnetic Field Configuration of a Filament Associated Flare from X-ray, UV and Optical Observations: C.C. Cheng, R. Pallavicini, Sol. Phys., 1984.

Energetics of a Compact Flare: Imlications for Flare Theory: J.G. Doyle and P.B. Byrne, Irish Astron. J., 1984, in press.

(b) Submitted or in Draft

Iron K-Alpha Emission Due to Non-Thermal Electrons in Solar Flares: A.G. Emslie and K.J.H. Phillips, draft.

X-Ray and Microwave Structures of a Limb Flare During the Impulsive Phase: G. Simnett, M.R. Kundu, E.J. Schmahl and K.T. Strong, draft, 1983.

Moving Noise Storm Radio Emission during the Early Stage of a Coronal Loop Transient: P. Lantos, and A. Kerdraon, draft.

Initial Phase of Chromospheric Evaporation in a Solar Flare: E. Antonucci and B.R. Dennis, A.H. Gabriel and G.M. Simnett, submitted to Sol. Phys.

Analysis of the Solar Flare of 7 April 1980 Based on SMM X-ray Data: B. Sylwester, J. Sylwester, J. Jakimiec, R. Mewe and R.D. Bentley, submitted to Sol. Phys., 1983.

Energetics of a Double Flare on November 8, 1980: J.G. Doyle, P.B. Byrne, B.R. Dennis, A.G. Emslie, A.I. Poland and G.M. Simnett, submitted to Sol. Phys., 1984.

A New Method for Determining Temperature and Emission Measure from Light Curves of Soft X-ray Line Fluxes: P.L. Bornmann, submitted to Astrophys. J., 1984.

Observation and Analysis of the Flare of 1700 UT, 12 November 1980: P. MacNeice, R. Pallavicini, H.E. Mason, G.M. Simnett, E. Antonucci, R.A. Shine, D.M. Rust, C. Jordan and B.R. Dennis, draft.

On Magnetic Field Stochaticity and Non-thermal Line Broadening in Solar Flares: E. Antonucci, R. Rosner, K. Tsinpanos, draft, 1984.

Results from the X-Ray Polychromator on SMM: J.L. Culhane, L.W. Acton, Mem. della Soc. Astron. Ital., draft, 1984.

III. CONFERENCE PROCEEDINGS

1979

A Two Axis Pointing System for an Orbiting Astronomical Instrument: R.F. Turner and J.G. Firth, Proc. 13th Aerospace Mechanisms Symposium (NASA Conf. Pub. 2031) JSC Houston, 26-27 April 1979.

1980

Preliminary Results from Ca and Fe Solar Flare Spectra from a Bent Crystal Spectrometer: E. Antonucci for XRP Team, College Park AAS Meeting, 1980.

Morphology of Active Regions and Flares: R.D. Bentley for XRP, College Park AAS Meeting, 1980.

Search for Flare Non-Thermal Electrons in Fe and Ca BCS Spectra: M.A. Kayat, A.H. Gabriel, K.J.H. Phillips for XRP Team, College Park AAS Meeting, 1980.

Dynamics of the High Temperature Flare: J.W. Leibacher for XRP Team, College Park AAS Meeting, 1980.

A Presentation of Some BCS Spectra: A. Parmar for XRP Team, College Park AAS Meeting, 1980.

Inner-Shell Ionization (K-alpha) Lines in Flare Impulsive Phases: K.J.H. Phillips for XRP & HXRBS Teams, College Park AAS Meeting, 1980.

Continuum Emission Observed with the BCS: C.G. Rapley for XRP & HXRBS Teams, College Park AAS Meeting, 1980.

Observations from the FCS on the SMM: K.T. Strong for XRP Team, College Park AAS Meeting, 1980.

Temporal Comparison of Fe K-alpha, & Hard X-Ray Emission During Several Solar Flares: C.J. Wolfson for XRP & HXRB Teams, College Park AAS Meeting, 1980.

Observational Insights Into Solar/Stellar Problems from the Solar Maximum Mission: L.W. Acton for SMM, NATO Advanced Study on Solar Phenomena in Stars and Stellar Systems, France.

Early Results from the SMM: C.G. Rapley on behalf of SMM Teams, IAU Colloquium No. 55, Toronto.

Preliminary Soft X-Ray Spectroscopy and Imagery from the SMM X-Ray Polychromator: J.W. Leibacher for XRP Team, IAU Colloquium No. 55, Toronto, 1980.

1981

Velocities Observed with the X-Ray Polychromator on Board the Solar Maximum Mission: J.W. Leibacher and XRP Team, AAS Solar Phys. Div., 1981 Meeting, Taos.

Changes in the Characteristics of the Coronal Plasma During Two Impulsive Flares: K.T. Strong, J. Sylwester, A. Parmar, B. Dennis, A. Poland and the XRP Team, AAS Solar Phys. Div., 1981 Meeting, Taos.

A Study of a Soft X-Ray Slow Event Associated with the Commencement of a Type 1 Noise Storm: C.G. Rapley, R.D. Bentley, P. Lantos, A. Kerdraon, AAS Solar Phys. Div., 1981 Meeting, Taos.

Coronal Flare Densities: C.J. Wolfson, J.G. Doyle, K.J.H. Phillips and XRP Team, AAS Solar Phys. Div., 1981 Meeting, Taos.

A Small Impulsive Flare: L.W. Acton, J.W. Leibacher and the XRP Team, AAS Solar Phys. Div. 1981 Meeting, Taos.

Soft X-Ray Emission During the Impulsive Phase of a Flare: E. Antonucci, A.H. Gabriel, J.G. Doyle and XRP Team, AAS Solar Phys. Div., 1981 Meeting, Taos.

Interpretation of the Ca XIX, Fe XXV, and Fe XXVI BCS Spectra: A.H. Gabriel, E. Antonucci, J. Dubau and XRP Team, AAS Solar Phys. Div., 1981 Meeting, Taos.

Control of the Soft X-Ray Polychromator on the Solar Maximum Mission Satellite: L.A. Springer, M. Levay, C.W. Gilbreth, M.L. Finch, R.D. Bentley and J.G. Firth, AIAA 19th Aerospace Science Meeting, St. Louis, 12-15 Jan. 1981.

Solar Flare Diagnostics Using the SMM: A.H. Gabriel, 1st European Conference on Atomic Physics. Heidelberg - April 1981.

Early Results from the XRP and UVSP Experiments on the SMM: A.H. Gabriel, Third European Solar Meeting of Solar Section, Astronomy and Astrophys. Division of EPS. Oxford, 1981.

Relationship Between a Soft X-Ray Long Duration Event and an Intense Noise Storm: C.G. Rapley, Third European Solar Meeting, Solar Section, Astronomy and Astrophys. Div. of EPS. Oxford, 1981.

The Excitation of Fe K-alpha Radiation in Flares: J.L. Culhane, Third European Solar Meeting, Solar Section, Astronomy and Astrophys. Div. of EPS. Oxford, 1981.

Analysis of the XRP Ca and Fe Spectra: J. Dubau, Third European Solar Meeting, Solar Section, Astronomy and Astrophys. Div. of EPS. Oxford, 1981.

Analysis of X-Ray Flare on 7 April 1980 Based on SMM Data: B. Sylwester, J. Sylwester, J. Jakimiec, R. Mewe, J. Schrijver, K.T. Strong, C. Rapley, Third European Solar Meeting, Solar Section, Astronomy and Astrophys. Div. of EPS. Oxford, 1981.

Determination of the Energy Balance During a Solar Flare, From Soft X-Ray Observations: N.J. Veck and C. Jordan, Third European Solar Meeting, Solar Section, Astronomy and Astrophys. Div. of EPS. Oxford, 1981.

Flare Densities from Iron K-alpha Lines: J.R. Lemen, K.J.H. Phillips and XRP Team, Bull. Am. Astr. Soc. 13, 543, 1981.

SMM Observations of Soft X-Ray Line Spectra: J.W. Leibacher, K.J.H. Phillips, C.J. Wolfson and XRP Team, Abstract in Bull. Am. Astr. Soc. 13, 555, 1981.

Analysis of Soft X-Ray Ca and Fe Spectra: M. Loulergue, L. Faucher, L. Steenman-Clark, European Phys. Soc. Meeting, Istanbul, Sept. 1981.

Analysis of X-Ray Spectra Emitted by High Temperature Plasmas: Solar Flares, Tokamak & Laser Fusion: F. Bely-Dubau and J. Dubau, European Phys. Soc. Meeting, Istanbul, Sept. 1981.

X-Ray Observations of Flares and Active Regions with the Flat Crystal Spectrometer on SMM: R. Pallavicini, G. Poletto and the XRP Team, Annual Meeting of Italian Astr. Soc. Modena, 1-4 Oct. 1981.

Hydrodynamics of Solar Flares: Observations and Numerical Modeling: R. Pallavicini, G. Peres, G. Vaiana and XRP Team, Annual Meeting of Italian Astr. Soc., Modena, 1-4 Oct. 1981.

Ground-Based and SMM Observations of a Filament-Associated Event on November 22, 1980: R. Pallavicini, L.W. Acton, C-C. Cheng, G. Nelson and A. Zappala, Annual Meeting of Italian Astr. Soc., Modena, 1-4 Oct. 1981.

Space-Borne and Ground-Based Observations of a Solar Active Region and a Flare: F. Chiuderi-Drago, Proceedings Vl ERMA Meeting, Dubrovnic, 1981.

SMM Soft X-Ray and UV Observataions of Solar Flares for the XRP Team, J.W. Leibacher, Tokyo, Nov. 1981.

X-Ray Classification of Flares in Large and Small Magnetic Structures: C.G. Rapley, RAS Discussion Meeting on Solar Flares, London, 11 Dec. 1981.

Soft X-Ray Discriminators of Flare Classifications: E. Antonucci, RAS Discussion Meeting on Solar Flares, London, 11 Dec. 1981.

Flare Classification - Fact or Fancy: L.W. Acton, RAS Discussion Meeting on Solar Flares, London, 11 Dec. 1981.

X-Ray Spectroscopic Observations from the Solar Maximum Mission - K.J.H. Phillips - Invited talk - Atomic Physics Conference, Baton Rouge, 1981. Abstract in Bull. Am. Phys. Soc.

Evidence for Simultaneous Presence of Large and Small Loops in Solar Flares: A.O. Benz, B.R. Dennis, J.W. Leibacher, R. Mewe, A. Poland, J. Schrijver, G. Simnett, J.B. Smith, K.T. Strong and J. Sylwester, Presented at IAU in Petrak, 1982.

Osservazioni SMM Radio and Ottiche di Regioni Attive Solar: E. Antonucci, R. Bandiera, F. Chiuderi-Drago and R. Falciani. SIF Meeting, Pisa 1981.

The XRP Experiment: E. Antonucci and C.J. Wolfson; Crimea SMM Workshop, March 1981.

1982

The Significance of Multiple Flares: K.T. Strong, B. Dennis, J.W. Leibacher, and C.J. Wolfson, Am. Astronomical Soc. Meeting, Boulder, 11-14 Jan. 1982.

Direct Evidence for Chromospheric Evaporation in a Well-Observed Compact Flare: R.C. Canfield, L.W. Acton, T.A. Gunkler, H.S. Hudson, A. Kiplinger and J.W. Leibacher, Am. Astronomical Soc. Meeting, Boulder, 11-14 Jan. 1982.

Direct Evidence for Chromospheric Evaporation in a Well Observed Compact Flare: R.C. Canfield, T.A. Gunkler, H.S. Hudson, L.W. Acton, J.W. Leibacher and A. Kiplinger, Symposium on SMY. COSPAR, Ottawa, 1982.

Observational Studies of Chromospheric Evaporation: L.W. Acton, Hinotori Symposium on Solar Flares, Jan. 1982.

Some Spectroscopic Results from the X-Ray Polychromator on SMM: K.J.H. Phillips, Hinotori Symposium on Solar Flares, Jan. 1982.

Correlations Between Soft X-Ray Long Duration Events and Metric Noise Storms: C.G. Rapley, Hinotori Symposium on Solar Flares, Jan. 1982.

1983

UV and X-Ray Observations of a Coronal Archade: K.T. Strong, M.E. Bruner, G. Poletto and R. Kopp. S.P.D. Meeting of Am. Astronomical Soc., Pasadena, June, 1983.

An X-Ray Empirical Model of a Solar Flare Loop: M. Bruner, W.A. Brown, L.W. Acton and K.T. Strong. S.P.D. Meeting of Am. Astronomical Soc., Pasadena, June, 1983.

The 12 November 1980 Flare at 17:00 UT: Analysis of Observations by the XRP, R. Pallavicini and L.W. Acton, UK SMM Workshop, May 1983.

1984

A New Method for Determining Temperature and Emission Measure Variations During Solar Flares: .L. Bornmann, Am. Astronomical Soc. Meeting, Baltimore, 11-13 June, 1984, abstract in Bull. Am. Astronomical Soc., 16, 545, 1984.

Variation in the Observed Coronal Calcium Abundance for Various X-ray Flare Plasmas: J.R. Lemen, J. Sylwester, R. Mewe., Am. Astronomical Soc. Meeting, Baltimore, 11-13 June, 1984, abstract in Bull. Am. Astronomical Soc., 16, 545, 1984.

Active Region Soft X-Ray Line Profiles: K.T. Strong, R.A. Stern, J.R. Lemen, and K.J.H. Phillips, Am. Astronomical Soc. Meeting, Baltimore, 11-13 June, 1984.

Recent Soft X-Ray Spectra During a Flare Decay: K.J.H. Phillips, J.R. Lemen, and K.T. Strong, Am. Astronomical Soc. Meeting, Baltimore, 11-13 June, 1984.

Filament Activations as Coronal Flare Precursors: D.F. Webb and E.J. Schmahl, Am. Astronomical Soc. Meeting, Baltimore, 11-13 June, 1984, abstract in Bull. Am. Astronomical Soc., 16, 536, 1984.

Electron Beam Heating during a Well-Observed Compact Flare: R.C. Canfield and T.A. Gunkler, Am. Astronomical Soc. Meeting, Baltimore, 11-13 June, 1984, abstract in Bull. Am. Astronomical Soc., 16, 544, 1984.

Soft X-Ray Spectroscopy from the X-Ray Polychromator on the Newly Repaired Solar Maximum Mission: K.T. Strong, J.R. Lemen, and K.J.H. Phillips, IAU Colloquium #86, Washington D.C., 27-29 August 1984.

New Calculations of Inner-Shell X-ray Lines in Ti, Cr, and Ni as Density Diagnostics: J.R. Lemen, K.J.H. Phillips, G.A. Doschek and R.D. Cowan, IAU Colloquium #86, Washington D.C., 27-29 August 1984.

Variation of the Observed Coronal Calcium Abundance for Various X-ray Flare Plasmas: J. Sylwester, J.R. Lemen and R. Mewe, IAU Colloquium #86, Washington D.C., 27-29 August 1984.

Derivation of the Ionization Balance for Fe XXIV / Fe XXV Using Solar X-ray Data: E. Antonucci, M.A. Dodero, A.H. Gabriel and K. Tanaka, IAU Colloquium #86, Washington, D.C., 27-29 August 1984.

IV. POPULAR ARTICLES

Solar Maximum Mission: E. Antonucci, L'Astronomie #16, 1982.

Las Fulguraciones Solares (Solar Flares): J.I. Garcia de la Rosa, F. Herrera and M. Vazques, Investigacion Y Ciencia #75, December 1982.

Stellar Coronas, X-rays and Einstein: R.A. Stern, Sky & Telescope, 68, 24-28, 1984.

V. TALKS

Soft X-Ray Line Spectra from SMM - J.W. Leibacher - Talk at Solar Neighborhood Meeting in Palo Alto, 13 Nov. 1981.

When the Sun Flares, All Hell Breaks Loose - L.W. Acton - Media talk at Lockheed Technology Symposium III, Washington, D.C., 16 Sept. 1981.

The Solar Flare Plasma Machine - L.W. Acton - Invited talk to Plasma Physics Division of American Physical Society, N.Y., 12 Oct. 1981.

Solar Flares Observed with the SMM - K.J.H. Phillips - Talk at Fitzharry's Astronomical Society, Abingdon, 9 Feb. 1982.

Observational Studies of Chromospheric Evaporation: L.W. Acton, Hinotori Symposium, Tokyo, 1982.

Some Spectroscopic Results From the X-Ray Polychromator on SMM: K.J.H. Phillips, Symposium on Hinotori and SMM Results, Tokyo, January 1982.

VI. POSTERS

Simultaneous Observations of AR2490 Performed in X-UV, Optical and Radio Wavelength Domain, Franca Chiuderi Drago, Solar Physics from Space Meeting, Zurich, 1980. Space Sci. Rev. 29, 439, 1981.

A Study of a Double Impulsive Flare Event: K.T. Strong, R. Mewe, B. Dennis, J.W. Leibacher, A. Parmar, A. Poland, J. Schrijver and J. Sylwester, Third European Solar Meeting, Solar Section, Astronomy and Astrophys. Div. of EPS. Oxford, 1981.

Bent Crystal Spectrometer Results on the Soft X-Ray Emission During the Impulsive Phase of Flares: E. Antonucci, Third European Solar Meeting of Solar Section, Astronomy and Astrophys. Division of EPS. Oxford, 1981.

Characteristics of the Soft X-Ray Long Duration Events Observed by the SMM X-Ray Polychromator: R.D. Bentley, C.G. Rapley and the XRP Team, AAS Solar Phys. Div., 1981 Meeting, Taos.

Analysis of XRP Bent Crystal Spectra of Hydrogen-Like Fe 26: A. Parmar, Third European Solar Meeting, Solar Section, Astronomy and Astrophys. Div. of EPS. Oxford, 1981.

Active Region Magnetic Fields: J.B. Smith, K.T. Strong, E. Schmahl, M. Kundu and R.D. Bentley, Am. Astronomical Soc. Meeting, Boulder, 11-14 Jan. 1982.

The Decay of a Large Limb Flare: P.J. Cargill, N.J. Veck, C. Jordan, K.T. Strong, G. Simnett and E.R. Priest. S.P.D. Meeting of Am. Astronomical Soc., Pasadena, June, 1983.

Recent Solar Observations from the X-Ray Polychromator on the Repaired SMM Satellite: J.L.R. Saba, G.L. Slater, M.X. Levay, K.L. Smith, K.T. Strong, R.D. Bentley, J.R. Lemen, R.R. Caffey, S.L. Freeland, D.P. Mathur, K.J.H. Phillips, and T.A. Waters, Am. Astronomical Soc. Meeting, Baltimore, 11-13 June, 1984.

Atomic Calculations for the Highly Ionized Iron Atoms Produced in Solar Flares: H.E. Mason and A.K. Bhatia, IAU Colloquium #86, Washington D.C., 27-29 August 1984.

APPENDIX B

SOLAR MAXIMUM MISSION
PRINCIPAL INVESTIGATORS: Dr. Loren W. Acton, LMSC
Lockheed Palo Alto Research Lab

Dr. J. Len Culhane, MSSL
Mullard Space Science Lab

Dr. Alan H. Gabriel, RAL
Rutherford Appleton Lab

XRP PROJECT SCIENTISTS:	Special Assignments
Dr. James R. Lemen, MSSL Dr. Keith T. Strong, LMSC Dr. Peter J. MacNeice, RAL Dr. Julia L. R. Saba, LMSC Dr. Ken J.H. Phillips, RAL	Plans daily XRP science operations in coordination with the other SMM scientists and the solar research community. Verifies the initial XRP operations analysis by the XRP Evaluator in conjunction with the XRP Engineer and the IOT Mgr. Conducts scientific analysis of XRP solar data in collaboration with the solar research community.

XRP INSTRUMENT OPERATION TEAM, (IOT):

IOT	SMM-II Job Titles	Job Functions
Michael Levay LMSC	IOT Manager Inst. Ops. Team	Manages the IOT. Provides expert analysis of the XRP instrument and micro-computer functioning and problems. Reprograms the XRP micro-computer.
Dnyanesh Mathur RAL	Engineering Programmer for XRP Operations.	Develops and maintains software for XRP Instrument Operations. Maintains the software library for XRP science analysis for LMSC, RAL, MSSL and the XRP-EOF.
Greg Slater ARC by LMSC	XRP Engineer	Provides detailed engineering evaluation and testing for operational management of the XRP instrument. Coordinates his activities with the Project Scientists and the IOT.
Samuel Freeland RAL	XRP Data Analyst Assistant Programmer	Provides preliminary evaluation of solar and XRP instrument data for the the Project Scientists and the XRP Engineer and the IOT Manager. Develops and maintains XRP software as directed by the XRP Programmer.

Teri Waters RAL	XRP Commander	Creates load directives for daily science and engineering plans. Codes XRP Sequences requested by the Project Scientist for science operation. Manipulates Real Time Sequences daily to support XRP Operational Plans. Maintains XRP Command Generation software for coded sequences. Verifies ground base software and spacecraft software match exactly.
Rebecca Coffey RAL	Prod. Data Processor Relief XRP Commander	Processes XRP Production Data Tapes. Maintains filing system for the processed XRP Production Data. Maintains expertise in Command Ops. for relief XRP Commanding.

Special Project	SMM-II Job	Job Functions:
Kermit Smith LMSC	Science Staff IOT Staff XRP Administrator	Provides XRP Project Scientists with science analysis of selected XRP solar X-ray events. Assists IOT as Relief Data Analyst. Oversees NOAA Flare Catalog for XRP. Establishes XRP-EOF equipment maintenance contracts. Interfaces officially for XRP with NASA-GSFC and LMSC.
Peter Waggett MSSL	Data Anal. Programmer Prod. Data Processor	Programmed IDL graphics software. Analyzed XRP solar white light images for the IOT.
Max Repace ARC by LMSC	Sci. Data Processor Asst. Programmer	Analyzes solar science data for the XRP Project Scientists. Creates software for delayed batch processing of XRP science data. Distributes NOAA solar data to RAL, MSSL, LMSC and the XRP-EOF.
Ben Brown PG Co. Schools by LMSC	Flare Cataloger Asst. IOT Member	Processes XRP solar flares for the NOAA computer flare catalog. Backs up DEC 11/34 Computer Sys. to magnetic tape on a monthly basis.

Orbit Number	Start GMT of Valid Data	BCS Sequence	FCS Sequence	Seq Ran	Det on	BCS max	Ca CR	COMMENTS
26748/49	1:20 (Full)	7.6-3.8e (54) 10.0.15.0 (2)	XTAL STARTUP 3'-5'-3'					ACTIVE REGION 4607
(49)	2:18 NIGHT	-						
26749/50	2:54 (Full)	"	XTAL STARTUP 3'-5'-3'					"
(50)	3:53 NIGHT	-	FRFNIGHT					
26750/51	4:29 (Full)	"	XTAL STARTUP 3'-5'-3'					"
(51)	5:27 NIGHT	-						
26751/52	6: 3 (Full)	"	XTAL STARTUP 3'-5'-3'					"
(52)	7: 2 NIGHT	-						
26752/53	7:37 (3/21/34)	"	7'X7' FRF7X7BP					"
(53)	8:36 NIGHT	-						
26753/54	9:12 (5/25/29)	"	7'X7' FRF7X7BP					"
(54)	10:10 NIGHT	-						
26754/55	10:46 (7/27/24)	"	7'X7' FRF7X7BP					"
(55)	11:45 NIGHT	-						
26755/56	12:21 (10/28/20)	"	4'X4'					"

Current Sequence in RTS 24: HP profiles at a point with triplet scans — ENABLED

Current Sequence in RTS 25: Crystal Drive Off - Chain to 4'(10") 0.62.37 — Priority Flag Set

```
                                BCS                              FCS

DATE              8/12/84       NORMAL/BACKUP = NORMAL           NORMAL/BACKUP = NORMAL
UT AT MF ZERO     0:11:40       MICRO STATUS  = RUN              MICRO MODE    = RUN
DAY OF YEAR   =     343         COMMAND STATUS=       0
FILE  NUMBER  =      10                                0         INTERPRETER ON? YES
MAJOR             438565        LOAD STATUS   =       6         TELEMETRY     = NSF
OBC SAA?          NO            SEQUENCE ID 10. 0.15.0          SEQUENCE ID   1.63.437
# HI VOLTS ON =       6         SEQNCE REPEAT =       7         SEQ RPTS LEFT =     126
SHARED TLM:       YES           MODE ID       =   16444         MODE ID             19536
                                MODE REPEAT   =      15         MODE RAN (SEC)      1047
                                FLARE?                74         GAS PUFF A    =   63483
                                MIN SINCE FLARE       64         GAS PUFF B    =    4153
OBC NIGHT?        YES           # OF CALS ON  =       0         CAL EXPOSED?      NO
                                TEST PULSER IS  OFF              TEST PULSER IS    OFF
                                SEQ INIT BY OBC                  XTAL DRIVE IS     OFF

 8/12/84   0:12: 4      OBC NIGHT?       B-ONLY      (F:10) (R:    5)
 8/12/84   0:12:12      # HI VOLTS ON =      10 <<<  (F:10) (R:    6)
 8/12/84   0:12:12      OBC NIGHT?       NO          (F:10) (R:    6)          FMS  REV 26671
 8/12/84   0:12:12  FCS SEQUENCE ID   1.63.506       (F:10) (R:    6)
 8/12/84   0:17:16  FCS TELEMETRY     = DTAF         (F:10) (R:   43)
 8/12/84   0:17:16  FCS SEQUENCE ID   1.63.437       (F:10) (R:   43)
 8/12/84   0:17:56  FCS INTERPRETER ON? NO           (F:10) (R:   48)
 8/12/84   0:21:29  FCS INTERPRETER ON? YES          (F:10) (R:   74)
 8/12/84   0:22: 2  FCS INTERPRETER ON? NO           (F:10) (R:   78)
 8/12/84   0:25:43  FCS INTERPRETER ON? YES          (F:10) (R:  105)
 8/12/84   0:26:16  FCS INTERPRETER ON? NO           (F:10) (R:  109)
 8/12/84   0:29:49  FCS INTERPRETER ON? YES          (F:10) (R:  135)
 8/12/84   0:29:57  FCS TELEMETRY     = NSF          (F:10) (R:  136)
 8/12/84   1:10:39  FCS SEQUENCE ID   1.63.506       (F:10) (R:  434)
 8/12/84   1:10:47      OBC NIGHT?       F-ONLY      (F:10) (R:  435)          LMS  REV 26671
 8/12/84   1:10:47  FCS INTERPRETER ON? NO           (F:10) (R:  435)
 8/12/84   1:10:55      OBC NIGHT?       YES         (F:10) (R:  436)
 8/12/84   1:11:52      # HI VOLTS ON =      12 <<<  (F:10) (R:  443)
 8/12/84   1:12: 1      # HI VOLTS ON =       6 <<<  (F:10) (R:  444)
 8/12/84   1:15:42  FCS TELEMETRY     = DTAF         (F:10) (R:  471)
 8/12/84   1:19:56  FCS INTERPRETER ON? YES          (F:10) (R:  502)
 8/12/84   1:19:56  FCS SEQUENCE ID   1.63.437       (F:10) (R:  502)
 8/12/84   1:20:37  FCS INTERPRETER ON? NO           (F:10) (R:  507)
 8/12/84   1:24:10  FCS INTERPRETER ON? YES          (F:10) (R:  533)
 8/12/84   1:24:42  FCS INTERPRETER ON? NO           (F:10) (R:  537)
 8/12/84   1:28:24  FCS INTERPRETER ON? YES          (F:10) (R:  564)
 8/12/84   1:28:24  FCS TELEMETRY     = NSF          (F:10) (R:  564)

 ***    1 Missing Major Frames ***

 ***    2 Missing Major Frames ***

END-OF-FILE ENCOUNTERED.    8/12/84   1:45:52  (F:10) (R:  689)
```

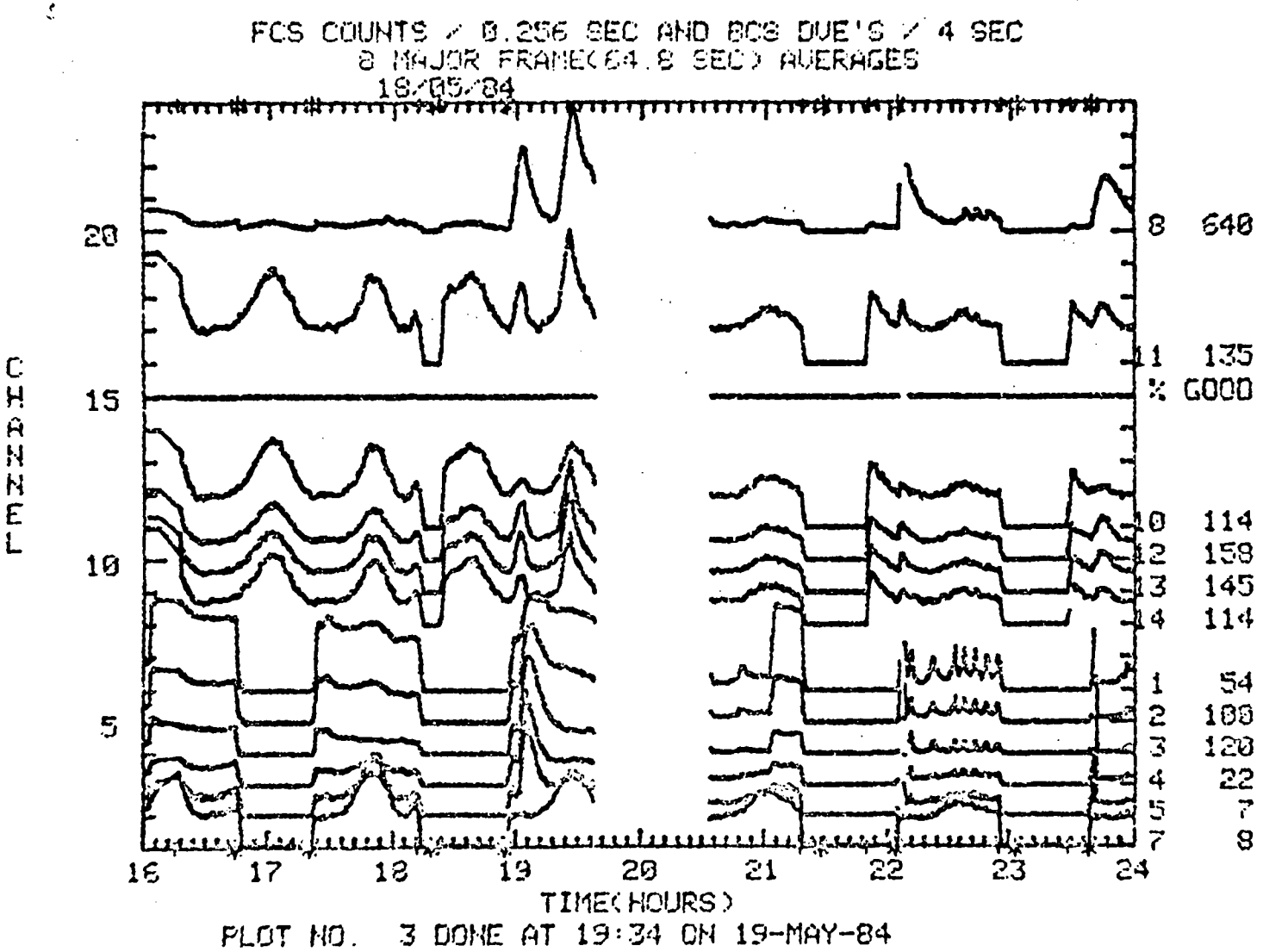
FCS COUNTS / 0.256 SEC AND BCS DUE'S / 4 SEC
8 MAJOR FRAME(64.8 SEC) AVERAGES
18/05/84
CHANNEL
20
15
10
5
8 640
11 135
% 6000
10 114
12 158
13 145
14 114
1 54
2 100
3 120
4 22
5 7
7 8
16
17
18
19
20
21
22
23
24
TIME(HOURS)
PLOT NO. 3 DONE AT 19:34 ON 19-MAY-84

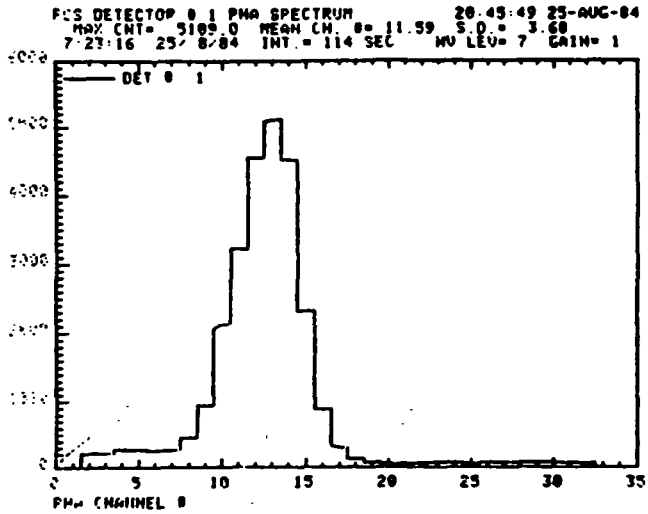
FCS DETECTOR # 1 PHA SPECTRUM
20:45:49 25-AUG-84
MAX CNT= 5109.0 MEAN CH. #= 11.59 S.D. = 3.60
7:23:16 25/ 8/84 INT.= 114 SEC HV LEV= 7 GAIN= 1
DET # 1
PHA CHANNEL #

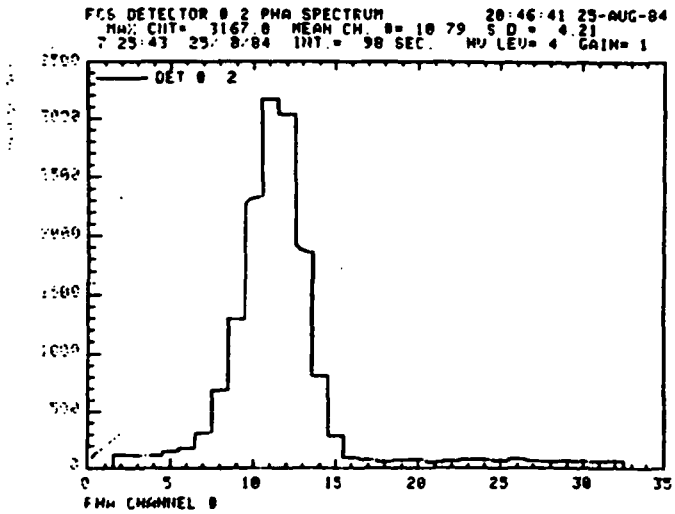
FCS DETECTOR # 2 PHA SPECTRUM
20:46:41 25-AUG-84
MAX CNT= 3167.0 MEAN CH. #= 10.79 S.D. = 4.21
7:25:43 25/ 8/84 INT.= 98 SEC. HV LEV= 4 GAIN= 1
DET # 2
PHA CHANNEL #

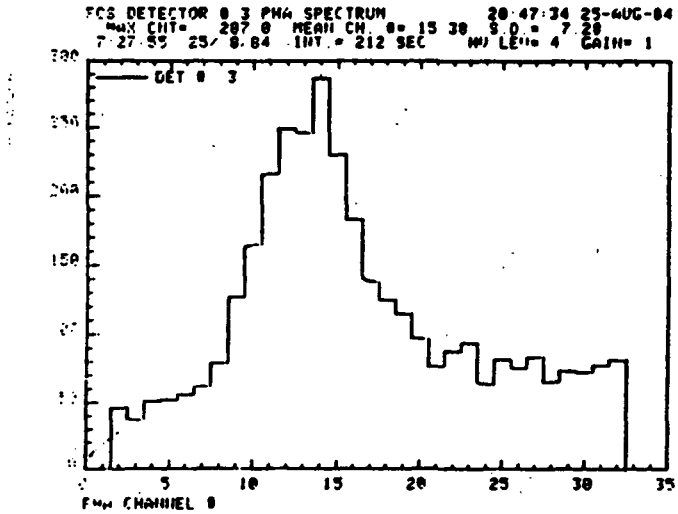
FCS DETECTOR # 3 PHA SPECTRUM
20:47:34 25-AUG-84
MAX CNT= 207.0 MEAN CH. #= 15.38 S.D. = 7.28
7:27:55 25/ 8/84 INT.= 212 SEC HV LEV= 4 GAIN= 1
DET # 3
PHA CHANNEL #

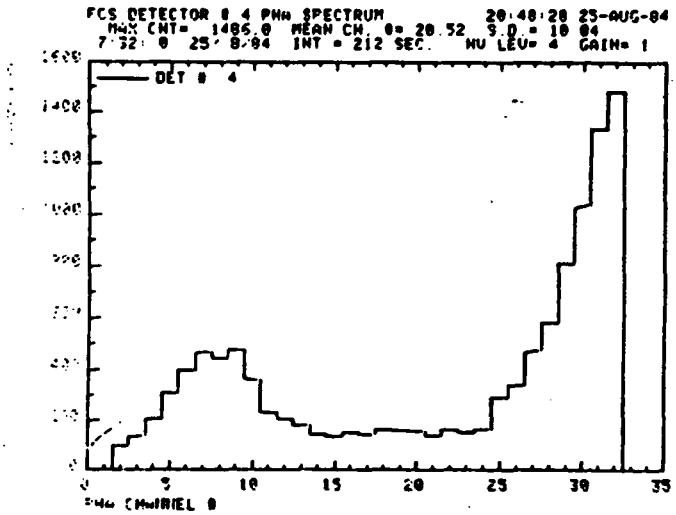
FCS DETECTOR # 4 PHA SPECTRUM
20:48:20 25-AUG-84
MAX CNT= 1486.0 MEAN CH. #= 20.52 S.D. = 10.84
7:32: 0 25/ 8/84 INT.= 212 SEC. HV LEV= 4 GAIN= 1
DET # 4
PHA CHANNEL #

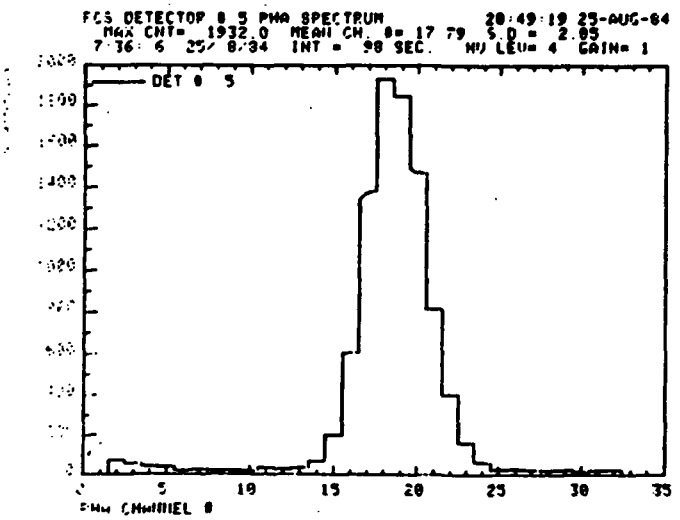
FCS DETECTOR # 5 PHA SPECTRUM
20:49:19 25-AUG-84
MAX CNT= 1932.0 MEAN CH. #= 17.79 S.D. = 2.85
7:36: 6 25/ 8/84 INT.= 98 SEC. HV LEV= 4 GAIN= 1
DET # 5
PHA CHANNEL #

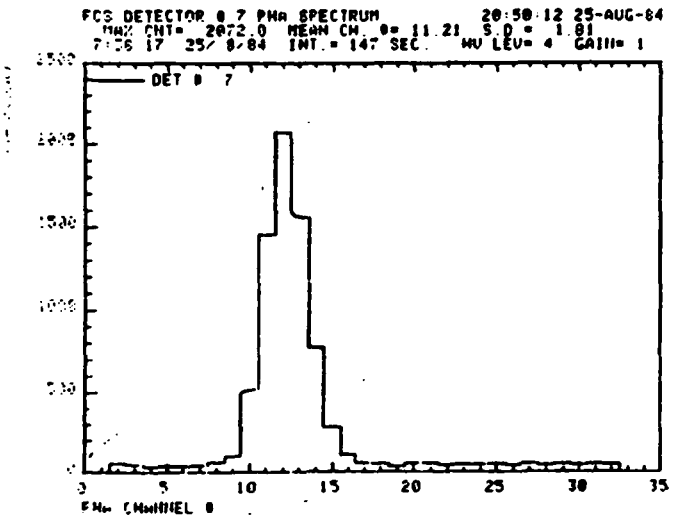
FCS DETECTOR # 7 PHA SPECTRUM
20:50:12 25-AUG-84
MAX CNT= 2072.0 MEAN CH. #= 11.21 S.D. = 1.81
7:36:17 25/ 8/84 INT.= 147 SEC. HV LEV= 4 GAIN= 1
DET # 7
PHA CHANNEL #

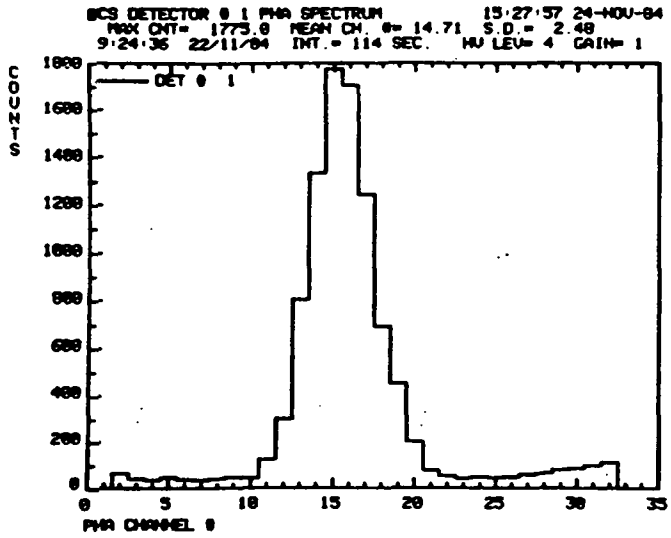
BCS DETECTOR 0 1 PHA SPECTRUM 15:27:57 24-NOV-84
MAX CNT= 1775.0 MEAN CH. 0= 14.71 S.D.= 2.48
9:24:36 22/11/84 INT.= 114 SEC. HV LEV= 4 GAIN= 1
DET 0 1
COUNTS
PHA CHANNEL 0

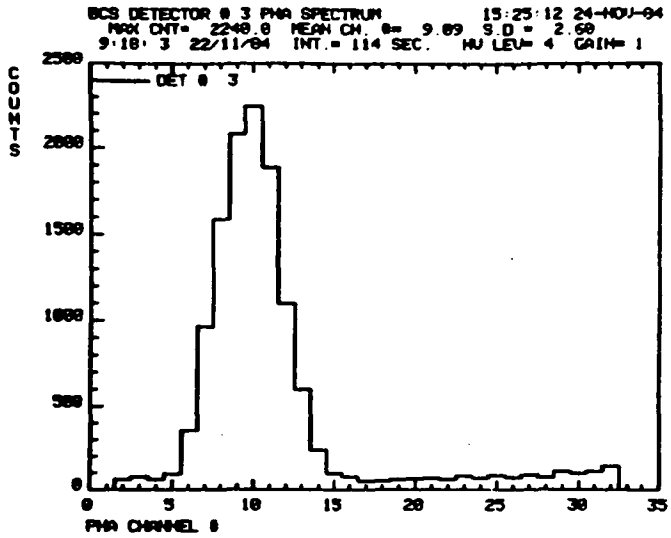
BCS DETECTOR 0 3 PHA SPECTRUM 15:25:12 24-NOV-84
MAX CNT= 2240.0 MEAN CH. 0= 9.09 S.D.= 2.60
9:18:3 22/11/84 INT.= 114 SEC. HV LEV= 4 GAIN= 1
DET 0 3
COUNTS
PHA CHANNEL 0

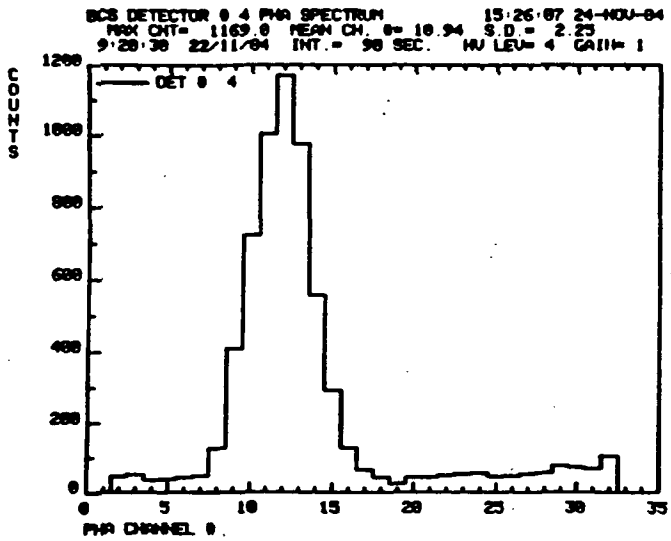
BCS DETECTOR 0 4 PHA SPECTRUM 15:26:07 24-NOV-84
MAX CNT= 1169.0 MEAN CH. 0= 10.94 S.D.= 2.25
9:20:38 22/11/84 INT.= 98 SEC. HV LEV= 4 GAIN= 1
DET 0 4
COUNTS
PHA CHANNEL 0

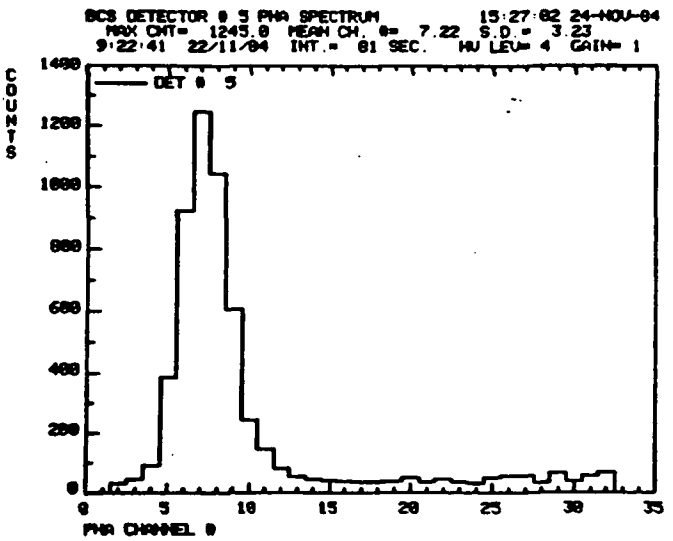
BCS DETECTOR 0 5 PHA SPECTRUM 15:27:02 24-NOV-84
MAX CNT= 1245.0 MEAN CH. 0= 7.22 S.D.= 3.23
9:22:41 22/11/84 INT.= 81 SEC. HV LEV= 4 GAIN= 1
DET 0 5
COUNTS
PHA CHANNEL 0

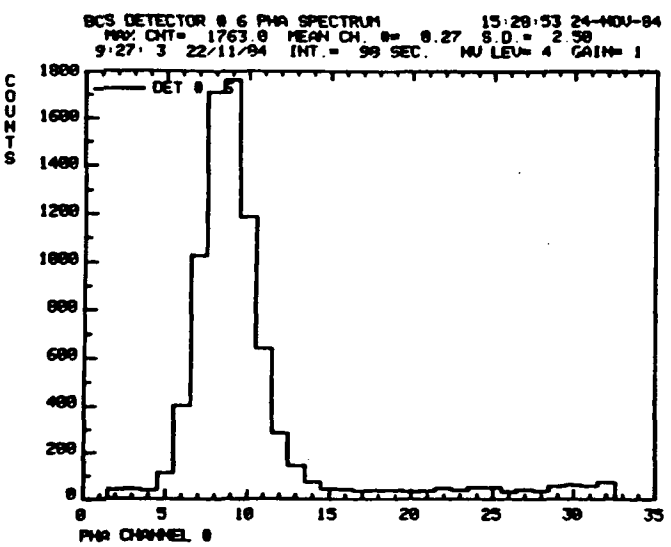
BCS DETECTOR 0 6 PHA SPECTRUM 15:29:53 24-NOV-84
MAX CNT= 1763.0 MEAN CH. 0= 8.27 S.D.= 2.58
9:27:3 22/11/84 INT.= 99 SEC. HV LEV= 4 GAIN= 1
DET 0 6
COUNTS
PHA CHANNEL 0

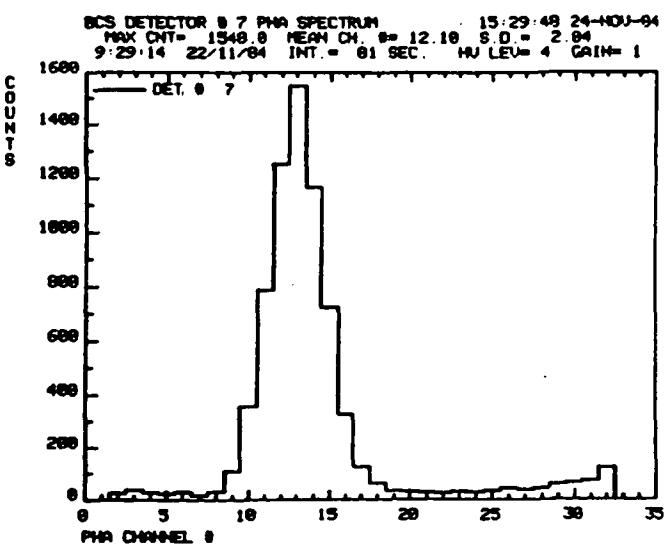
BCS DETECTOR 0 7 PHA SPECTRUM 15:29:48 24-NOV-84
MAX CNT= 1548.0 MEAN CH. 0= 12.10 S.D.= 2.84
9:29:14 22/11/84 INT.= 81 SEC. HV LEV= 4 GAIN= 1
DET 0 7
COUNTS
PHA CHANNEL 0

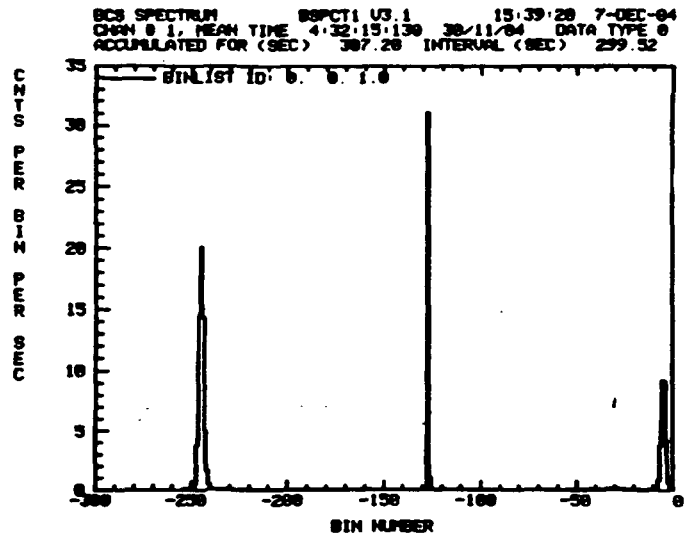
BCS SPECTRUM BSPCT1 V3.1 15:39:20 7-DEC-84
CHAN 0 1, MEAN TIME 4:32:15:130 30/11/84 DATA TYPE 0
ACCUMULATED FOR (SEC) 307.20 INTERVAL (SEC) 299.52
BINLIST ID: 0. 0. 1.0
CNTS PER BIN PER SEC
BIN NUMBER

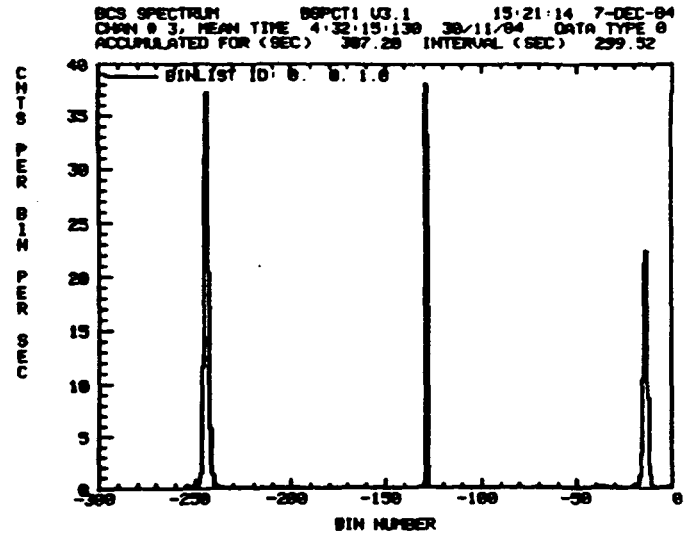
BCS SPECTRUM BSPCT1 V3.1 15:21:14 7-DEC-84
CHAN 0 3, MEAN TIME 4:32:15:130 30/11/84 DATA TYPE 0
ACCUMULATED FOR (SEC) 307.20 INTERVAL (SEC) 299.52
BINLIST ID: 0. 0. 1.0
CNTS PER BIN PER SEC
BIN NUMBER

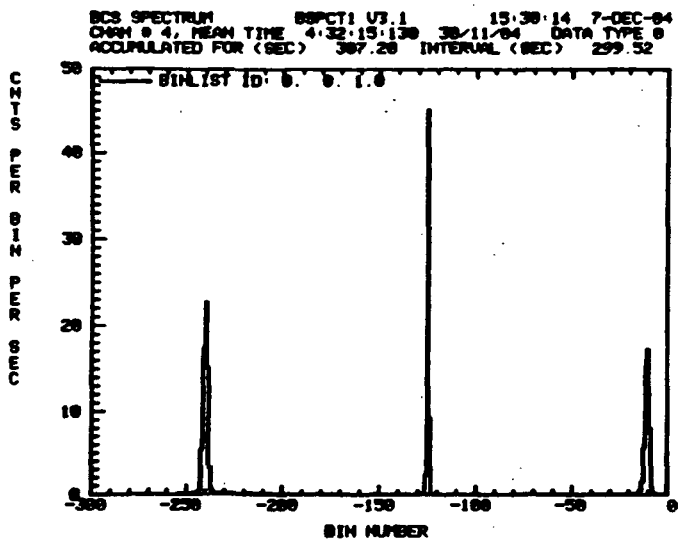
BCS SPECTRUM BSPCT1 V3.1 15:30:14 7-DEC-84
CHAN 0 4, MEAN TIME 4:32:15:130 30/11/84 DATA TYPE 0
ACCUMULATED FOR (SEC) 307.20 INTERVAL (SEC) 299.52
BINLIST ID: 0. 0. 1.0
CNTS PER BIN PER SEC
BIN NUMBER

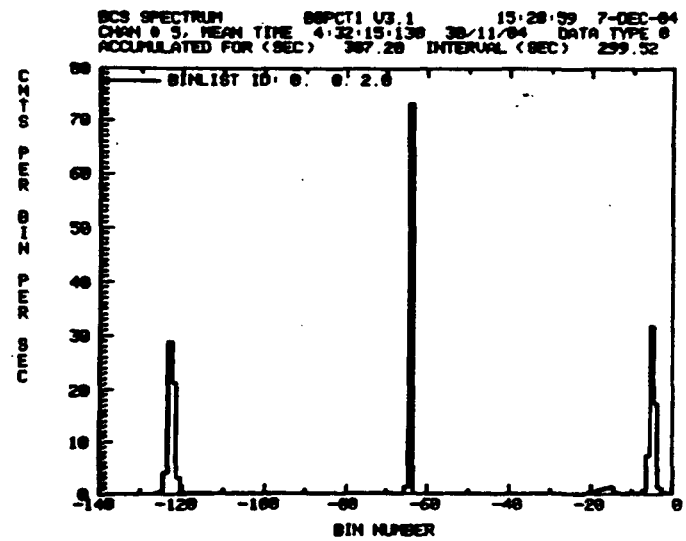
BCS SPECTRUM BSPCT1 V3.1 15:28:59 7-DEC-84
CHAN 0 5, MEAN TIME 4:32:15:130 30/11/84 DATA TYPE 0
ACCUMULATED FOR (SEC) 307.20 INTERVAL (SEC) 299.52
BINLIST ID: 0. 0. 2.0
CNTS PER BIN PER SEC
BIN NUMBER

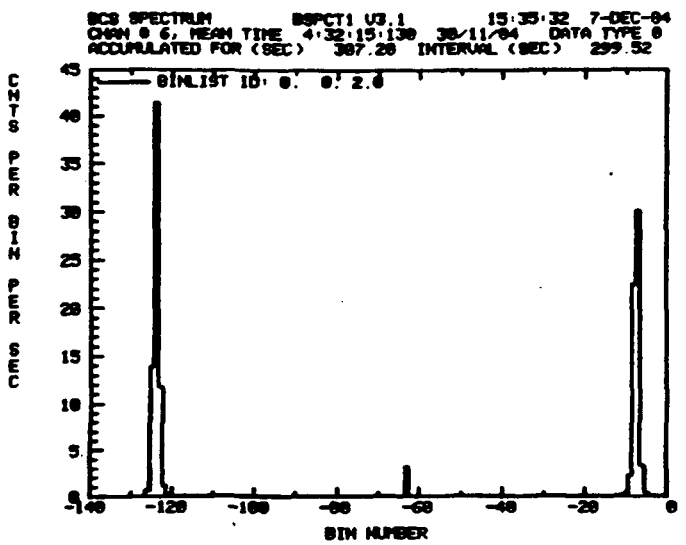
BCS SPECTRUM BSPCT1 V3.1 15:35:32 7-DEC-84
CHAN 0 6, MEAN TIME 4:32:15:130 30/11/84 DATA TYPE 0
ACCUMULATED FOR (SEC) 307.20 INTERVAL (SEC) 299.52
BINLIST ID: 0. 0. 2.0
CNTS PER BIN PER SEC
BIN NUMBER

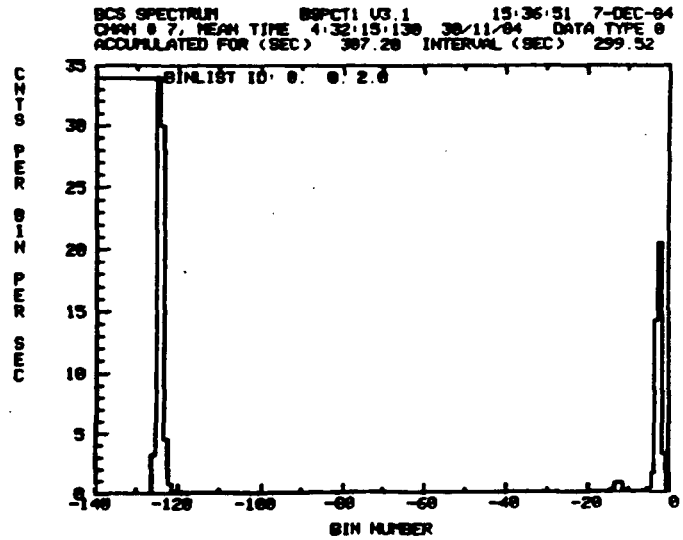
BCS SPECTRUM BSPCT1 V3.1 15:36:51 7-DEC-84
CHAN 0 7, MEAN TIME 4:32:15:130 30/11/84 DATA TYPE 0
ACCUMULATED FOR (SEC) 307.20 INTERVAL (SEC) 299.52
BINLIST ID: 0. 0. 2.0
CNTS PER BIN PER SEC
BIN NUMBER

All other detectors off

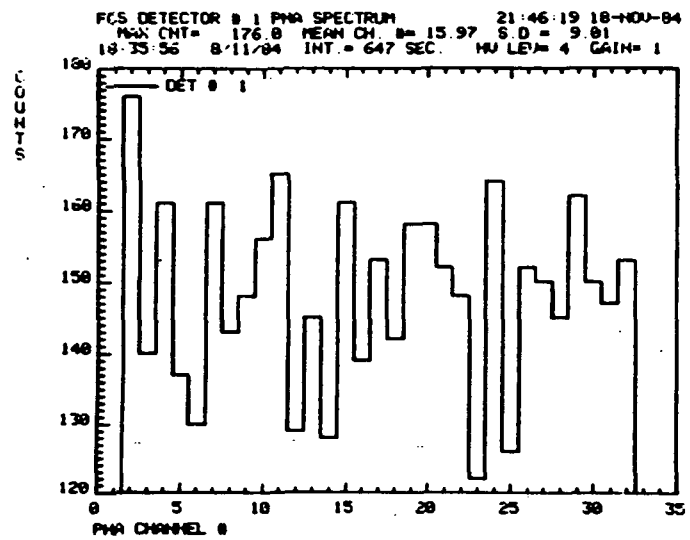

All other detectors on

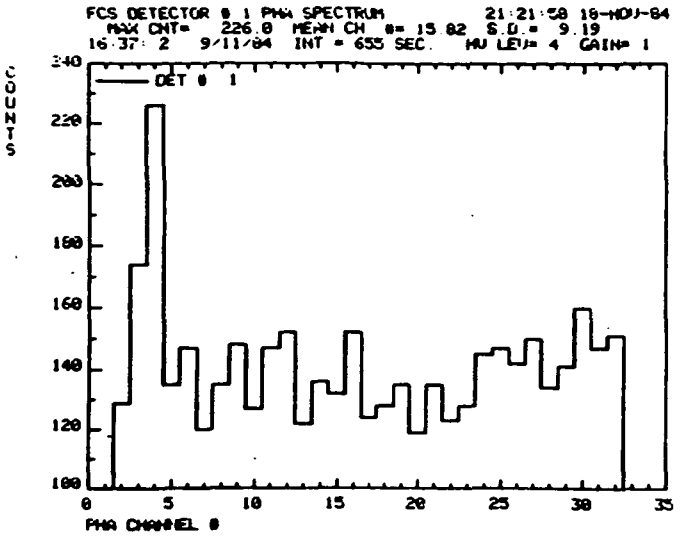

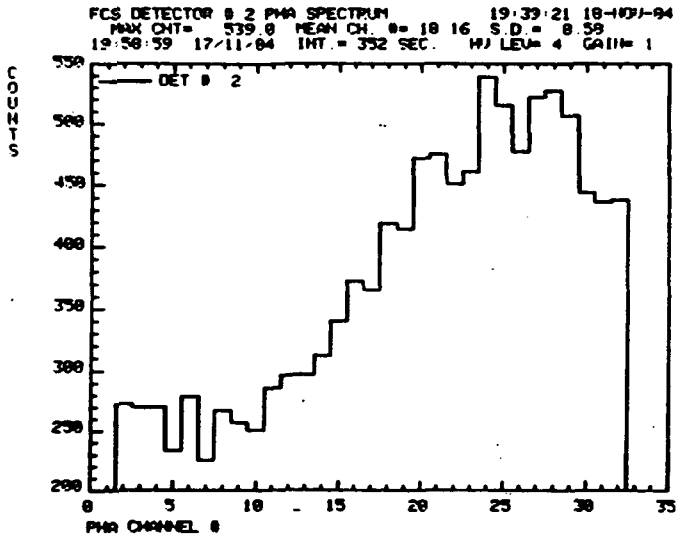

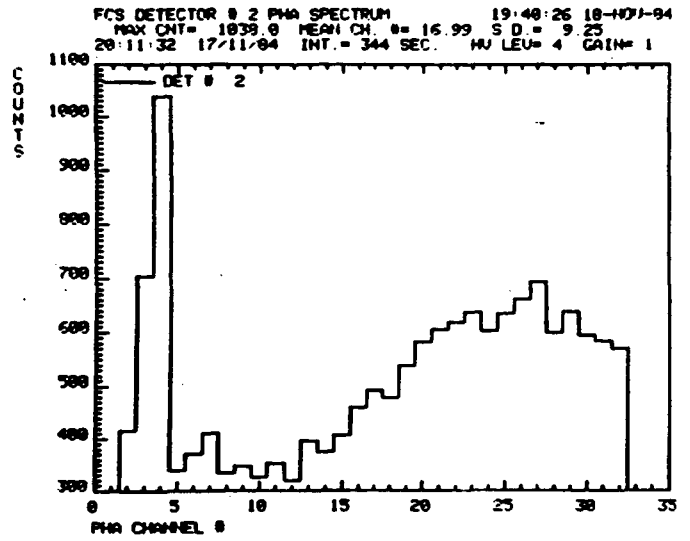

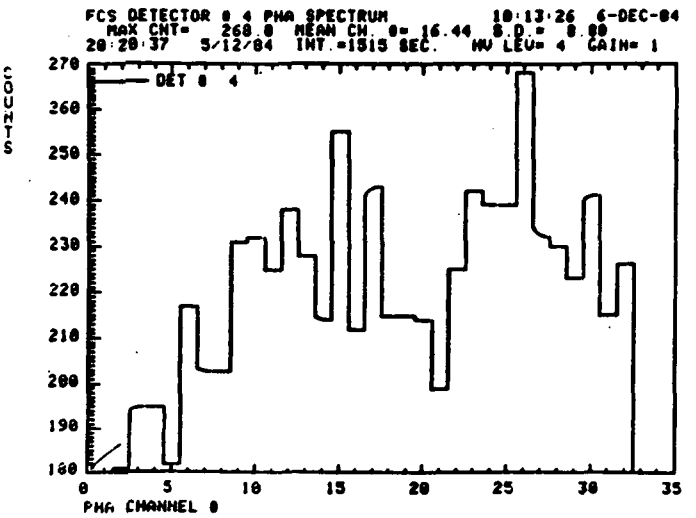

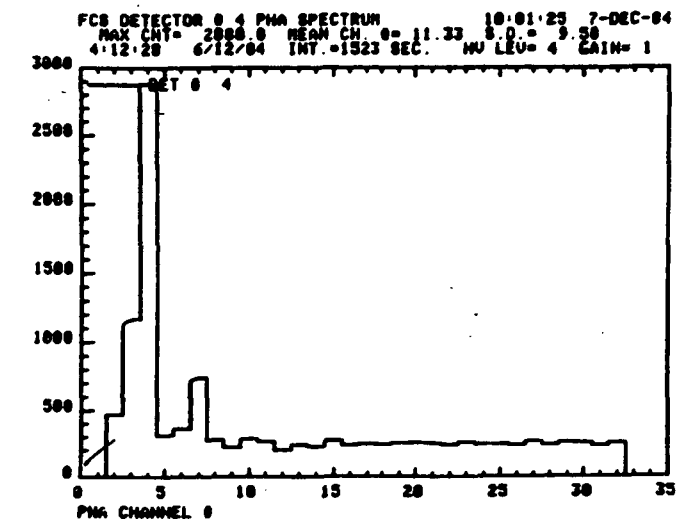

RASTER SLIPS - 1984 (PAGE 5)

OPS DATE	GM TIME	Y SAE/TRANS	Z SAE/TRANS	MAGNITUDE OF SLIP	SLIP DURATION (IN MINS.)	SEQ/RTS AND RASTER MOTION IDS
6/13	00:39:41	150/134	75/69	4	16	FRFWANGG
6/13	01:03:35	182/172	75/69	36	29	FRFWANG2
6/13	02:07:04	142/123	75/69	16	7	062093 & 062094
6/13	02:14:10	140/124	75/69	16	16	FRFWANGG
6/13	02:30:25	138/122	75/69	16	8	GAP
6/13	02:38:12	125/107	75/69	30	63	FRFWANGG
6/13	03:41:25	142/119	75/69	20	7	062093 & 062094
6/13	08:24:43	152/137	80/63	4	24	062093 (4/7X10, 0/10X0)
6/13	03:48:39	99/76	75/69	60	92	FRFWANGG
6/13	11:40:55	152/138	81/62	8	17	FRFWANGG
6/13	11:33:41	152/137	80/62	8	23	062093-(4/7X10, 0/10X0)
6/13	22:42:01	148/133	75/69	4	68	FRFWANGG
6/16	04:05:30	152/137	83/59	8	23	062093 (4/7X10, 0/10X0)
6/16	04:28:51	154/138	77/67	4	60	062093 (4/7X10, 0/10X0)
6/16	05:39:59	152/137	77/66	4	24	062093 (4/7X10, 0/10X0)
6/16	07:14:20	152/137	79/64	4	23	062093 (4/7X10, 0/10X0)
6/16	11:57:38	152/138	79/65	4	23	062093 (4/7X10, 0/10X0)
6/16	22:58:36	152/137	83/59	8	23	062093 (4/7X10, 0/10X0)
6/17	17:51:33	152/138	99/38	32	7	062093 (4/7X10, 0/10X0)

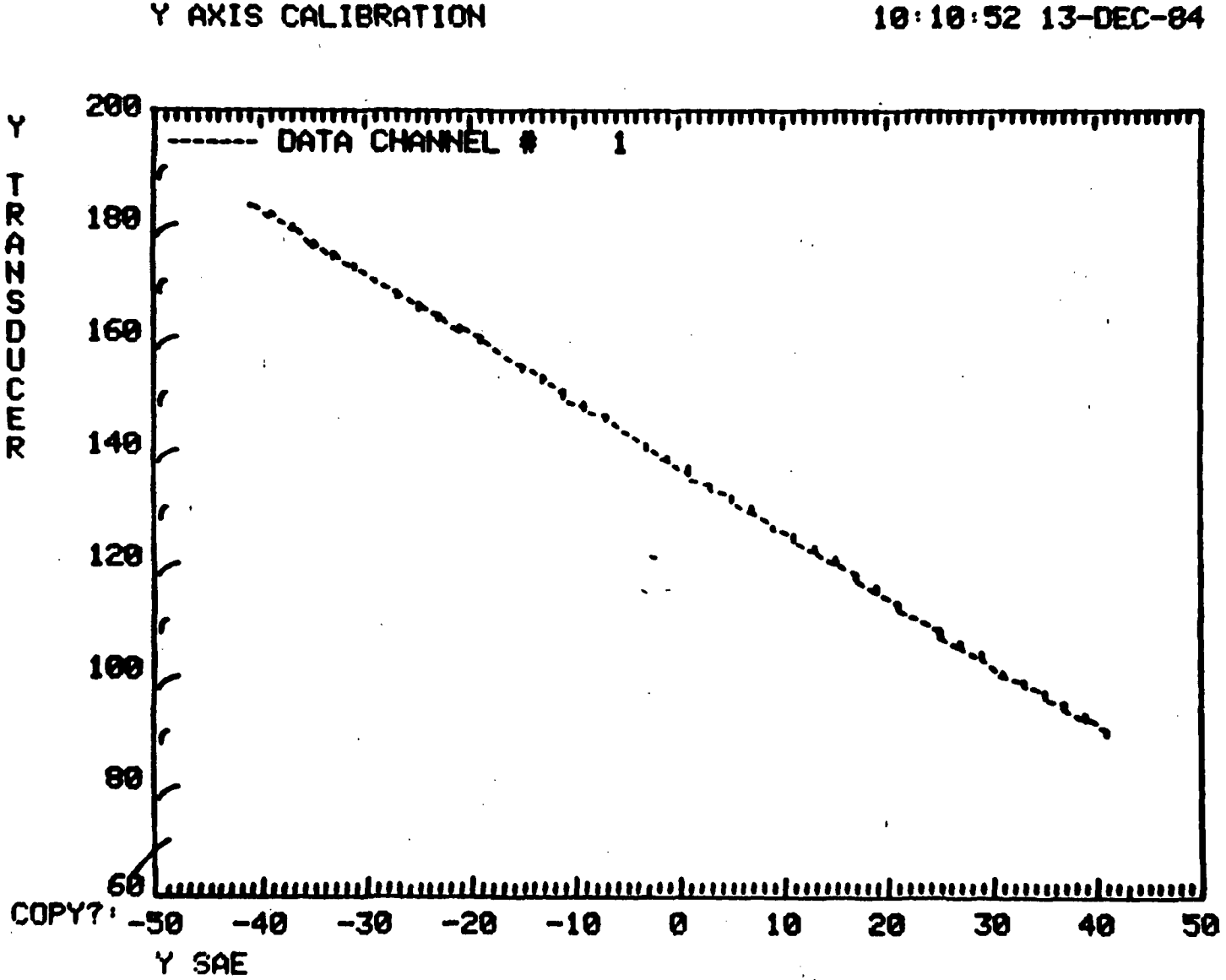
Y AXIS CALIBRATION
10:10:52 13-DEC-84
------ DATA CHANNEL # 1
Y TRANSDUCER
200
180
160
140
120
100
80
60
COPY?:
-50
-40
-30
-20
-10
0
10
20
30
40
50
Y SAE

8

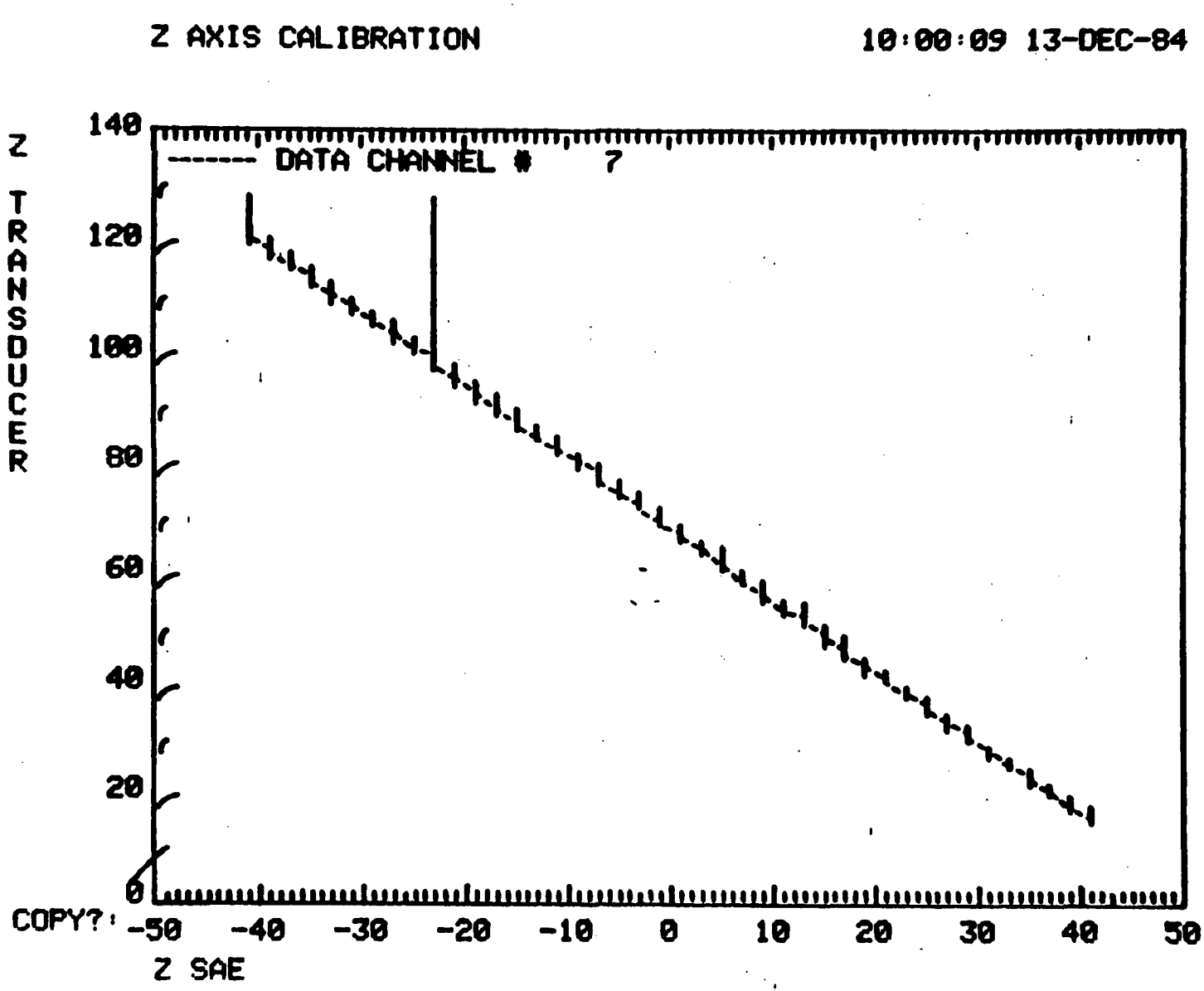
Z AXIS CALIBRATION
10:00:09 13-DEC-84
------ DATA CHANNEL # 7
Z TRANSDUCER
140
120
100
80
60
40
20
0
COPY?
-50
-40
-30
-20
-10
0
10
20
30
40
50
Z SAE

CRYSTAL DRIVE USE LOG

Date	Time	Initial Address	Crys. Temp. At On	Duration	Running Total	Total Post Repair	Sequence	Address Range	No. of Flybacks	No. of Misreads
11/ 3/80	22:43	6353		~ 0	0		Test			
1/ 8/80		6356		1:	1:		Check out			
25/ 8/80	13:02	6356		28:	29:		Real Time			
4/ 9/80	22:03	6355		1:	30:		To Cal			
8/ 9/80		13822		1:	31:		To HP			
16/ 9/80	22:10	6355		4:	35:		Real Time			
23/ 9/80	20:14	6358		10:	45:		0.61.7			
25/ 9/80	20:00			1:	46:		0.61.8x3			
22/10/80	16:33	6354		3:	49:		Real Time			
5/11/80	22:29	6354		15:15	64:15		0.61.10			
		6353		15:15	79:30		0.61.10			
11/11/80	2:04	6355		0:30	80:00		Real Time			
11/11/80	16:27	6364		0:30	80:30		Real Time			
13/11/80	23:65	6358		1:00	81:30		Real Time			
		6368					Real Time			
9/ 6/83	22:11	6358		5:18	86:48					
16/ 6/83	22:39			7:14	94:02					
28/ 4/84	21:22-21:35			12:42	1:46:44	12:42	PHA Cal			0
28/ 4/84	21:35-21:53	6353		21:10	2:07:54	33:52	———			0
28/ 4/84	21:53-22:56	6353	16.8,18.0	59:29	3:07:23	1:33:21	0.61.90	6280-6430	192	0
30/ 4/84	18:02-19:01	6357	15.6,16.3	58:31	4:05:54	2:31:52	0.61.91	6310-7030	32	0
1/ 5/84	21:58-22:12	6356		13:42	4:19:36	2:45:34	PHA Cal			0
2/ 5/84	22:00-22:58	6356	16.1,16.8	57:40	5:17:16	3:43:14	0.61.024	762-1284	4	0
								6130-7570	4	
								2200-2700	4	
								3906-4467	4	
								2200-2770	1	
								3906-4467	1	
13/ 5/84	15:46-15:59			12:33	5:29:49	3:55:47	PHA Cal			0
17/ 5/84	18:57-19:14			17:37	5:47:26	4:13:24	PHA Cal			0
19/ 5/84	15:26-16:22	6357	15.1,15.8	60: ?	6:47:26	5:13:24	0.61.93(32)	6310-7030	32	0
21/ 5/84	14:46- ?	6358	14.5,15.4	60: ?	7:47:26	6:13:24	0.61.93(32)	6310-7030	32	0
25/ 5/84	15:51-16:09	6359		8:55	7:56:21	6:22:19	PHA Cal			0
26/ 5/84	13:19-13:41	6359	15.1,15.9	21:16	8:17:37	6:43:35	0.61.092	6280-6430	192	10
6/ 6/84	2:54- 3:10		15.2,16.1	15:42	8:33:19	6:59:17	1.63.418	1400-1500	20	0
								1900-2000	20	
								2400-2500	20	
								2900-3000	20	
								3400-3500	20	
								3900-4000	20	
								4400-4500	20	
								4900-5000	20	
								5400-5500	20	
								5900-6000	20	
								6400-6500	20	
								6900-7000	20	
								7400-7500	20	
								7900-8000	20	
								8400-8500	20	
								8900-9000	20	
24/ 8/84	~14:08-14:09	6358		~ 1	8:34:19	7:00:17	To Cal			0
26/ 8/84	19:21-19:26	13822		4:39	9:13:58	7:04:56	To 6145			0
27/ 8/84	02:03-02:05	6171		1:54	9:15:52	7:06:50	To Home			0
20/ 9/84	17:26:18:20	6357	17.0,17.7	54:26	10:10:18	8:01:16		6320-6415	576	7

ADDITIONAL NOTES

Date	Time	Comments
28/ 4/84	21:22-21:35	FCS PHA Cal attempt. Failed.
28/ 4/84	21:35-21:56	Drive left on between PHA Cal and sequence 0.61.90.
28/ 4/84	21:56-22:56	
30/ 4/84	18:02-19:01	
1/ 5/84	21:58-22:12	FCS PHA Cal attempt. Failed.
2/ 5/84	22:00-22:58	
13/ 5/84	15:46-15:59	
17/ 5/84	18:57-19:14	
19/ 5/84	15:26-16:22	
21/ 5/84	14:46- ?	Incomplete data. (Zero misreads seen.)
25/ 5/84	15:51-16:09	
26/ 5/84	13:19-13:41	First evidence of irregularities in flyback profiles.
6/ 6/84	2:54- 3:10	J. Sherman's drive test sequence. No slips. However, in the 6400-6500 sweeps, overshoots of 7 to 15 address units consistently occurred.
26/ 8/84	19:21-19:26	Attempt to return crystal to home. Command error resulted in final address of 6145.
27/ 8/84	2:03- 2:05	Crystal sent to proper address this time (6353).

SYSTEM A GAS USAGE (GM) AS OF 5-12-84 IS:

PRESSURE DECAY METHOD: 847.3
PUFF COUNT METHOD: 956.4

SYSTEM A REMAINING GAS (GM):

PRESSURE DECAY METHOD: 1152.7
PUFF COUNT METHOD: 1043.6

SYSTEM A OPERATIONAL LIFETIME (MONTH) AT CURRENT LOW PRESSURE LEAK RATE:

PRESSURE DECAY METHOD: 36.9
PUFF COUNT METHOD: 31.3

SYSTEM A MASS LOSS RATE (GM/SEC) AVERAGED OVER LATEST ON PERIOD:

PRESSURE DECAY METHOD: 0.118E-04
PUFF COUNT METHOD: 0.126E-04

SYSTEM B GAS USAGE (GM) AS OF 5-12-84 IS:

PRESSURE DECAY METHOD: 1354.2
PUFF COUNT METHOD: 1475.1

SYSTEM B REMAINING GAS (GM):

PRESSURE DECAY METHOD: 645.8
PUFF COUNT METHOD: 524.9

SYSTEM B OPERATIONAL LIFETIME (MONTH) AT CURRENT LOW PRESSURE LEAK RATE:

PRESSURE DECAY METHOD: 6.7
PUFF COUNT METHOD: 3.1

SYSTEM B MASS LOSS RATE (GM/SEC) AVERAGED OVER LATEST ON PERIOD:

PRESSURE DECAY METHOD: 0.368E-04
PUFF COUNT METHOD: 0.656E-04

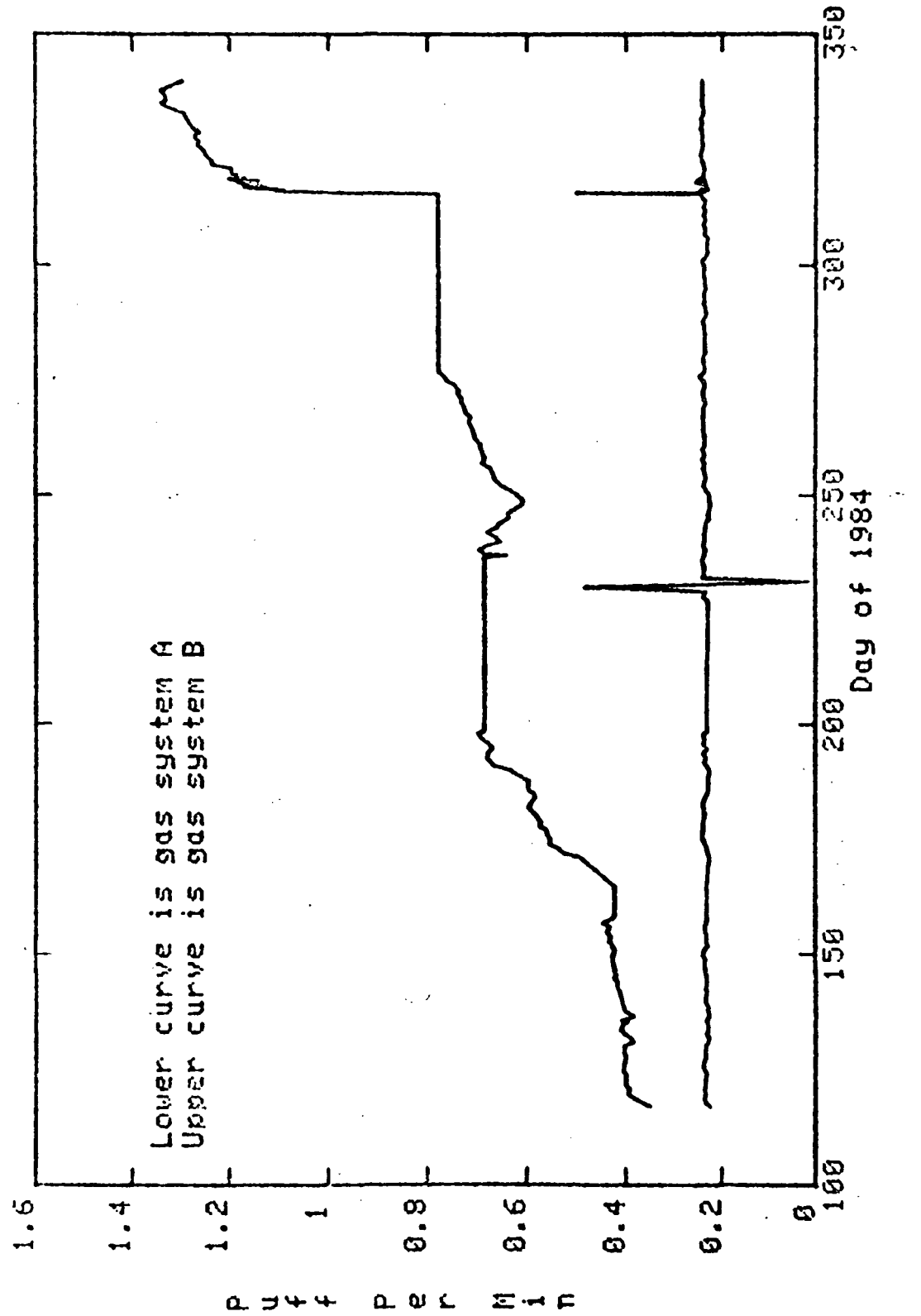
Lower curve is gas system A
Upper curve is gas system B
puff per Min
Day of 1984
1.6
1.4
1.2
1
0.8
0.6
0.4
0.2
0
100
150
200
250
300
350

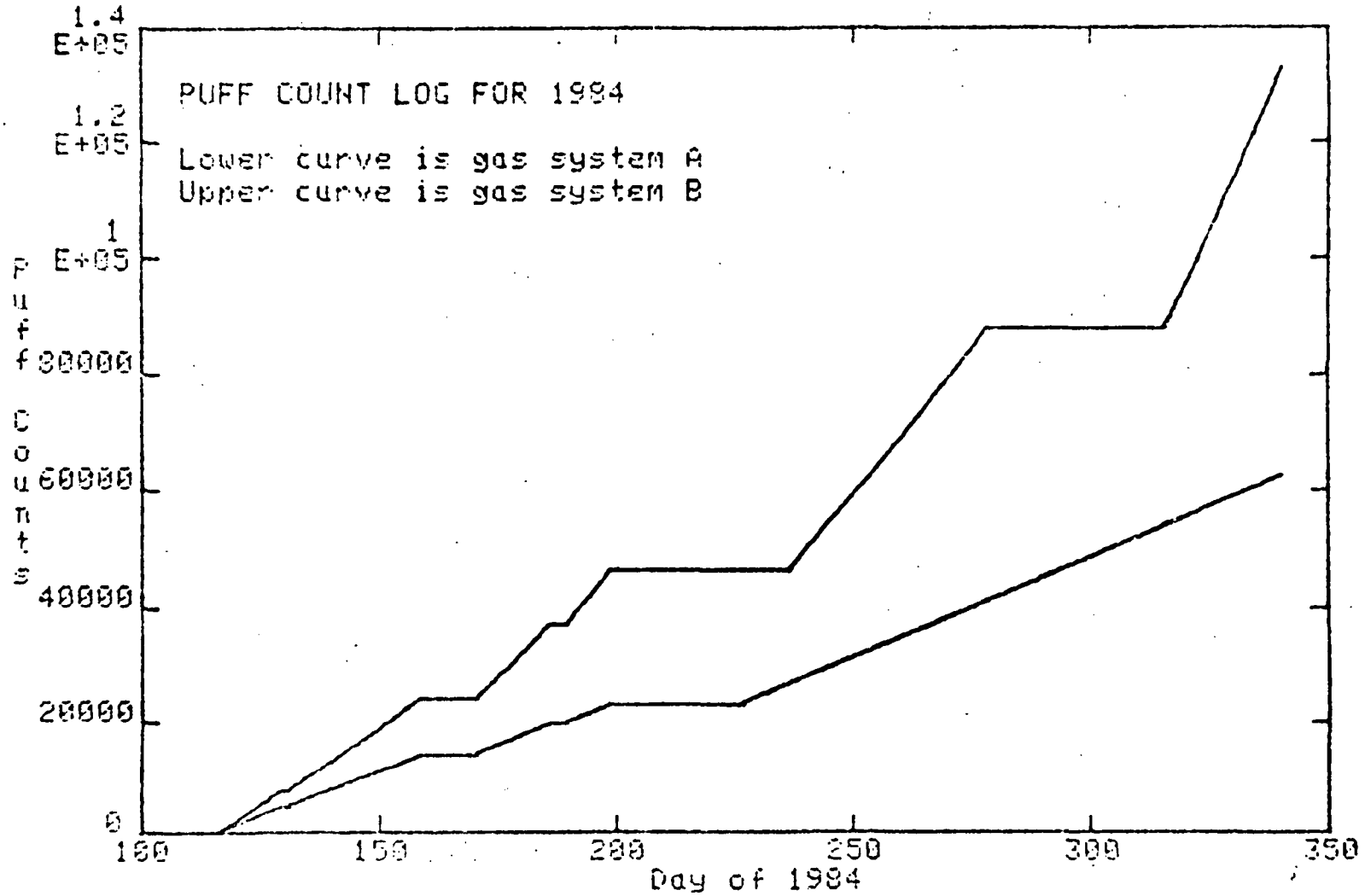
PUFF COUNT LOG FOR 1984
Lower curve is gas system A
Upper curve is gas system B
Puff Counts
1.4 E+05
1.2 E+05
1 E+05
80000
60000
40000
20000
0
100
150
200
250
300
350
Day of 1984

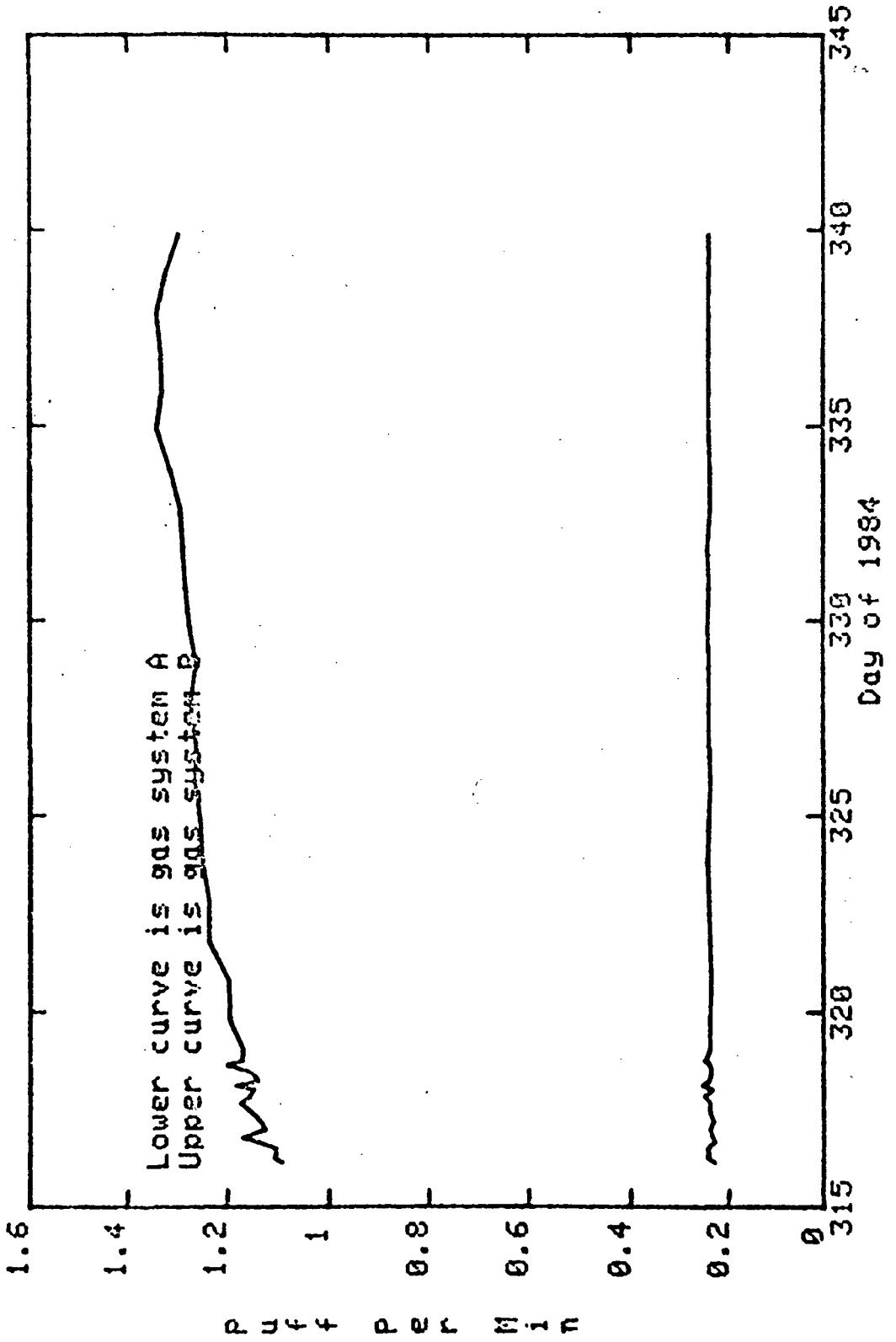
Lower curve is gas system A
Upper curve is gas system B
Puff per Min
1.6
1.4
1.2
1
0.8
0.6
0.4
0.2
0
315
320
325
330
335
340
345
Day of 1984

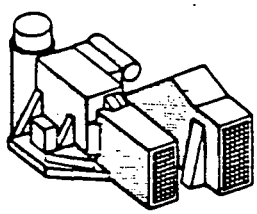

7 Dec. 1984
Kermit L. Smith
(301)344-8279
(301)344-7557 ANS. Mach.

X-RAY POLYCHROMATOR
SOLAR MAXIMUM MISSION

CODE 602.6 (BLDG. 7, XRP) GODDARD SPACE FLIGHT CENTER GREENBELT, MD. 20771
TELEPHONE (301) 344-7557 TELECOPY: (301) 344-6230 TWX: 89675

XRP's WEEKLY ACTIVITY REPORT of 7 Dec. 1984

1. TOTAL XRP INSTRUMENT STATUS:

* Sys. A Gas Supply Remaining: 31 to 37 months.
* Sys. B Gas Supply Remaining: 3.1 to 6.7 months. Leak rate increases while on.
* Sys. B was shut off 6 Dec.'84 to conserve gas until next solar activity.
  Gas Sys. B's Exponential Decay to be used to improve Remaining Gas Estimate.

* The BCS Detector System has no operational problems and is working well.

* Several misreads occurred during last usage of the FCS XTAL Drive on 20 Sept.
  FCS XTAL Drive Bulb B is degrading in same manner as old Bulb A.
  FCS XTAL Drive Bulb B has an estimated lifetime of 200 hours actual usage.

* The Alignment Sensors are all working properly with stable responses.

2. IOT ACTIVITIES, PROBLEMS and PLANS:

* The serious FCS Raster Drive slipping problems in Y-axis started 9 Nov.'84.
  The FCS Raster Drive slippage problem is improving somewhat, but very slowly.
  Alternate FCS Cam Set to be tested while work continues on Primary Cam Set.

3. CALIBRATIONS, ETC.:

* SNEW Slews are scheduled weekly.

4. ADMINISTRATIVE ISSUES WITH NASA:

* SMM's Bldg. 7 power will be shut off on the last two Dec. '84 weekends.!
* Old April-May 1984 XRP Merged Production Tapes are arriving by the box load.

5. PROGRESS on SCIENCE OBSERVING PLANS:

* The Sun remains very quiet, and no coronal hole is on the disk this week.

* A Region "behind" the East limb had several small flares in a 6 hour period.
  The XRP East Limb Survey had mapped the Region. The Region died on disk.

6. SMM-WIDE OPERATIONAL ISSUES:

* "Comments on SL2 and SMM" of 5 Dec.'84 by L.W. Acton has been distributed.
* SL2 now officially scheduled for 22 June, already slipping towards 26 June.

7. POLITICS, VISITS, & RUMORS:

* John Parkinson visited XRP this week.
* Keith Strong returns from Calif. on 7 Dec. 1984.
* Kermit Smith will spend the Christmas Holidays in California.

APPENDIX C : DATA SUBMISSION PLAN FOR THE NATIONAL SPACE SCIENCE DATA CENTER

The X-ray Polychromator experiment consists of two instruments, the Bent Crystal Spectrometer (BCS) and the Flat Crystal Spectrometer (FCS). The complete data set from both of these experiments is presently accessible at the SMM Data Analysis Center (DAC) through the use of the extensive package of analysis software developed for our own use. The DAC represents our primary archival submission of this data set. We have provided both personnel and hardware towards the establishment of the DAC and are prepared to continue to work with the NSSDC to provide data to outside users so long as our level of analysis support permits this additional service activity.

As we have discussed at length, the permanent archiving of the XRP data set in a scientifically useful form requires essentially the capability of the DAC and is beyond the scope and resources of the NSSDC. Therefore, for the foreseeable future the NSSDC/DAC cooperation appears to be the best solution to fulfilling the charter obligations of the NSSDC to see that SMM data are available to the general user community. The extremely non-homogeneous nature of this data set (many instrument modes, variable solar conditions, substantial number of instrument maladies, etc.) makes bulk reduction and archiving excessively costly. Furthermore, the most valuable research aspects of the data set would have to be comprised in the necessary selection and editing to make the volume of "reduced" data manageable for the NSSDC.

The XRP related materials most suited for NSSDC archiving fall into two categories. The first provides information on the mission as a whole and, incidently, important XRP data.

1. SMM pointing log.
2. Solar Maximum Mission Active Region Histories and Synoptic Observations.
3. Solar Maximum Mission Event Listing.
4. Daily planning log produced by the SMM planning chief.

We assume that the NSSDC already has these materials. If not, the project scientist can readily provide them as they are already in finished form.

The second category of the XRP materials provide information on the nature and quality of XRP data and the XRP observing mode(s). The materials have some limited value for research but are mostly useful for deciding whether to look into the primary data base. The materials we propose to provide the NSSDC are the following:

1. Annotated catalog of all XRP data describing time of running and nature of each observing sequence, orbital sunrise and sunset, entrance and exit from SAA, SMM pointing, etc. This can be delivered as hardcopy or on magnetic tape.

2. Counting rate plots of all 15 XRP data channels (15 Channel Light Curves), 12 hours per page, for the useful life of the mission. These show instantly whether flares were observed at any given time and provide considerable information on what the XRP was doing and the statistical success of the experiment. These would be delivered on hard copy.

3. Ca XIX counting rate curves and sample eight channel spectra for all flares observed with the BCS which are intense enough to be statistically significant. This represents about 300 flares and would be delivered on hard copy.

We would propose to deposit these materials, along with appropriate documentation including published papers describing the XRP, with the NSSDC. Transfer of additional material to the NSSDC upon shut down of the DAC will represent additional effort not covered under the present contract.